

The green box: an electronically versatile perylene diimide macrocyclic host for fullerenes

Timothy A. Barendt,^{*,†} Stuart P. Cornes,[‡] Maria A. Lebedeva,^{†,‡} William K. Myers,[§] Kyriakos Porfyrakis,[‡] Igor Marques,[¶] Vítor Félix,[¶] and Paul D. Beer^{*,†}

[†]Chemistry Research Laboratory, Department of Chemistry, University of Oxford, Mansfield Road, Oxford OX1 3TA, United Kingdom

[§]Centre for Advanced ESR, Inorganic Chemistry Laboratory, Department of Chemistry, University of Oxford, South Parks Road, Oxford OX1 3QR, United Kingdom

[‡]Department of Materials, University of Oxford, Parks Road, Oxford OX1 3PH, United Kingdom

[¶]Department of Chemistry, CICECO – Aveiro Institute of Materials, University of Aveiro, Aveiro, Portugal

ABSTRACT: The powerful electron accepting ability of fullerenes makes them ubiquitous components in biomimetic donor-acceptor systems that model the intermolecular electron transfer processes of Nature's photosynthetic centre. Exploiting perylene diimides (PDIs) as components in cyclic host systems for the non-covalent recognition of fullerenes is unprecedented, in part because archetypal PDIs are also electron deficient, making dyad assembly formation electronically unfavourable. To address this, we report the strategic design and synthesis of a novel large, macrocyclic receptor comprised of two covalently strapped electron-rich bis-pyrrolidine PDI panels, nicknamed the "Green Box" due to its colour. Through the principle of electronic complementarity, the Green Box exhibits strong recognition of pristine fullerenes ($C_{60/70}$), with the non-covalent ground and excited state interactions that occur upon fullerene guest encapsulation characterised by a range of techniques including electronic absorption, fluorescence emission, NMR and time-resolved EPR spectroscopies, cyclic voltammetry, mass spectrometry and DFT calculations. Whilst relatively low polarity solvents result in partial charge transfer in the host donor-guest acceptor complex, increasing the polarity of the solvent medium facilitates rare, thermally allowed full electron transfer from Green Box to fullerene in the ground state. The ensuing charge separated radical ion paired complex is spectroscopically characterised, with thermodynamic reversibility and significant kinetic stability also demonstrated. Importantly, the Green Box represents a seminal type of $C_{60/70}$ host where electron-rich PDI motifs are utilised as recognition motifs for fullerenes, facilitating novel intermolecular, solvent tuneable ground state electronic communication with these guests. The ability to switch between extremes of the charge transfer energy continuum is without precedent in synthetic fullerene-based dyads.

Introduction

Beyond their aesthetic appeal, fullerenes possess intriguing electrochemical, photophysical and magnetic properties^{1,2} with a wide variety of applications stemming from photovoltaics^{3–5} and superconductors^{6–8} to biological^{9–11} and organic electronics.^{12–15} Within the latter, the renowned electron accepting ability¹⁶ and small reorganisation energy¹⁷ of rigid, symmetric fullerenes has led to their combination with electron donors to generate elegant models of Nature's photosynthetic reaction centre,¹⁸ that capture, transform and store energy via electronic donor–acceptor interactions.^{1,19} Such dyads have been constructed from covalent^{12,20–22} and mechanical bonds,^{23–28} however, a non-covalent approach^{15,29–31} is particularly desirable because it follows biomimetic principles of design whilst also preserving the singular electronic properties of fully conjugated cages such as pristine C_{60} and C_{70} fullerenes.³² Therefore, in conjunction with supramolecular chemistry, a range of synthetic receptors^{33–53} have been developed with the large cavities of preorganized macrocyclic hosts often providing the optimum strategy in terms of affinity and selectivity for fullerenes in solution.^{54,55} Hosts containing electron rich, lipophilic cavities are also preferential, on the basis of electronic complementarity towards the electron deficient fullerene guest, enabling interactions to be visualized spectroscopically.^{54,56} When these criteria are satisfied intermolecular partial charge transfer in the ground state and/or full single electron transfer (SET) in the excited state can occur between donor and acceptor.^{34,36,42,44} However, thermally promoted SET in the ground state, an extreme of the charge transfer energy continuum,^{57–59} is, to the best of our knowledge, unprecedented in a rationally designed fullerene-based dyad system.

Perylene diimides (PDIs) represent a class of chemically, thermally and photophysically stable organic dye molecules.^{60–62} Their rich photo- and electrochemistry provides a wide range of visible light absorptions, characteristic long lived

excited states and the ability to undergo efficient energy and electron transfer reactions, making them ideal components in synthetic donor–acceptor assemblies.^{63–68} However, the covalent^{69–85} or non-covalent^{37,86,87} linking of PDI derivatives with C₆₀ fullerene has generated dyads in which negligible electron communication has been observed spectroscopically in the ground state^{37,69–76,79,80,86–88} whilst energy transfer was the predominant relaxation pathway for the excited state.^{70–72,74,76,79,83,87} This is because, like fullerenes, archetypal PDIs are benchmark electron deficient aromatic molecules.⁶⁰ Fortunately, their electronic properties can be modulated such that the incorporation of electron-donating pyrrolidine heterocycles in two of the bay positions of the perylene core causes a large, negative shift in oxidation potential to produce an electron-rich PDI.⁸⁹ Furthermore, these chromophores are green with large extinction co-efficients in the highly desirable red and NIR regions, where a significant fraction of the solar spectrum occurs.⁹⁰ While two previously reported dyads comprised of a bis-pyrrolidine PDI and a covalently appended C₆₀ fullerene exhibit photoinduced electron transfer from donor to acceptor,^{82,88} spectroscopic evidence for strong electronic communication between these motifs in the ground state remains elusive, and host–guest non-covalent systems are unprecedented. Furthermore, thermally promoted SET between a PDI motif and fullerene remains unknown.

Herein we describe the rational design, synthesis and fullerene recognition properties of a large, macrocyclic receptor comprised of two covalently strapped electron-rich bis-pyrrolidine PDI panels, nicknamed the “Green Box” due to its colour. These PDI chromophores were chosen because: (i) they provide electronic complementarity to electron-deficient fullerene guests; (ii) the bis-bay substituted PDI aromatic framework is twisted and flexible⁹⁰ to allow optimization of alignment/intimate contact with the curved surface of a fullerene⁹¹ and (iii) they are monomeric, exhibiting excellent solubility in organic solvents. Furthermore, aryl and alkyl spacer units were used in tandem to create a macrocyclic host with a preorganised, lipophilic cavity, whilst also maintaining some flexibility for structurally idealised guest encapsulation (size/shape complementarity). Novel ground and excited state electronic interactions between the macrocycle’s PDI components and pristine C_{60/70} fullerene guest species are demonstrated via a non-covalent approach.⁹¹ We have employed a range of spectroscopic and electrochemical techniques to comprehensively characterise the fullerene recognition properties of Green Box, **4**, and its impact on the electronics of host and guest. For the first time, this work reveals a fullerene-based dyad with solvent tuneable partial charge ($[4]^{\delta+} \rightarrow [C_{60/70}]^{\delta-}$) or full electron transfer ($[4]^{++} \rightarrow [C_{60/70}]^{--}$) in the ground state of the supramolecular complex assembly (Figure 1).

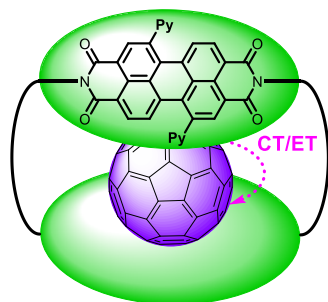
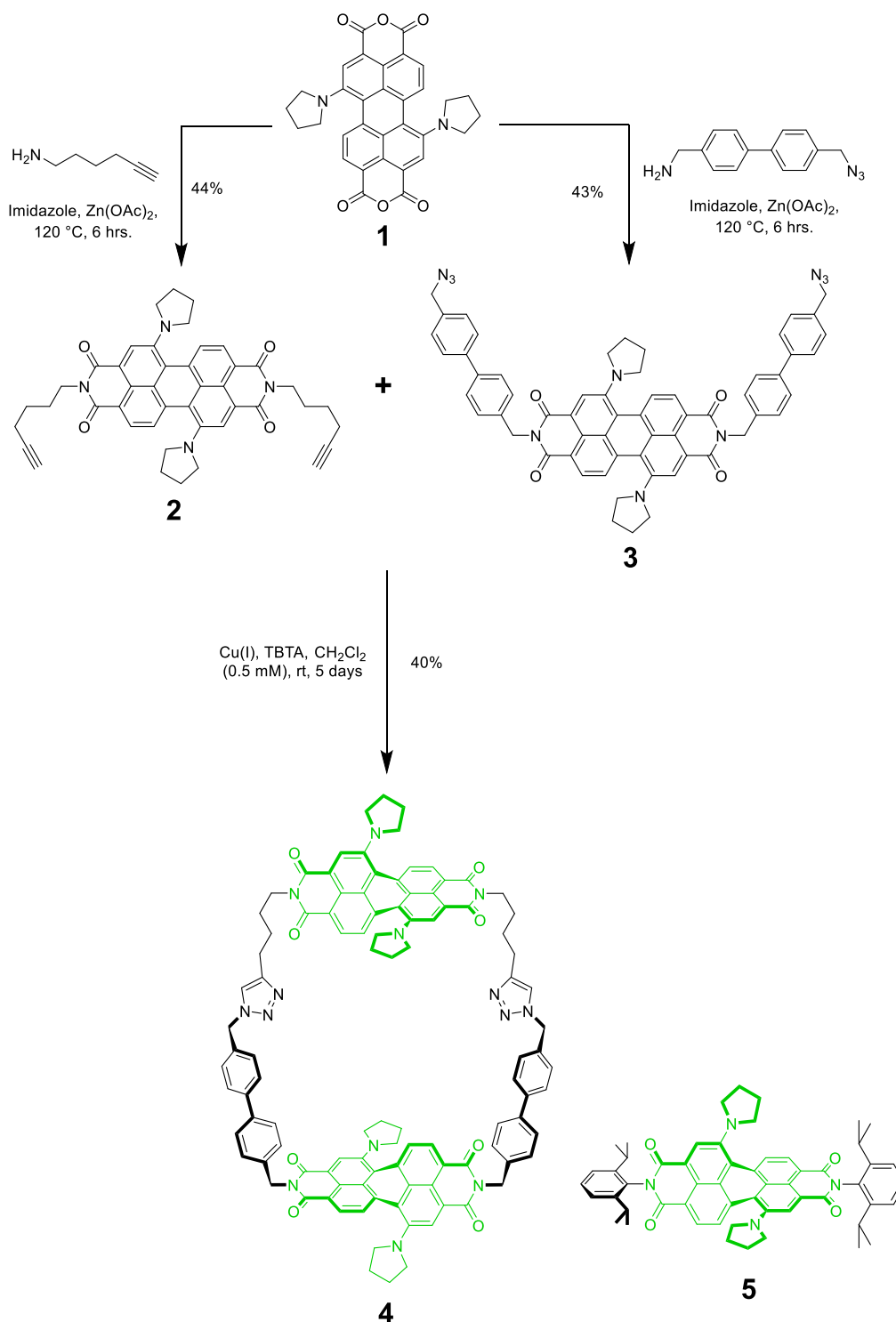


Figure 1. Schematic of pristine fullerene recognition inside the electron rich cavity of a bis-pyrrolidine PDI macrocycle (Green Box) and electronic communication in the host donor–guest acceptor complex. (CT = ground state partial charge transfer, ET = ground or excited state full electron transfer, Py = pyrrolidine).

Synthesis and Characterisation

The Green Box bis-PDI macrocycle **4** was prepared by a multi-step synthetic pathway as fully described in the Supporting Information (Scheme 1 and Supporting Information section 1). Initially, bis-pyrrolidine perylene-3,4,9,10-tetracarboxylic dianhydride (PTCDA)⁹² **1** was synthesised in four steps as the pure C1,7 bay-functionalised regioisomer, whilst condensation with an appropriate amine^{93,94} afforded bis-pyrrolidine perylene-3,4,9,10-tetracarboxylic diimide (PDI) derivatives containing either butyl alkyne (**2**) or a biphenyl azide (**3**) at each of the imide termini. A [1+1] macrocyclization reaction was then performed with these precursors via a double copper(I)-catalyzed azide alkyne cycloaddition (CuAAC) “click” reaction under high dilution conditions (0.5 mM) to give the large bis-peryene diimide-containing macrocycle **4** as a dark green solid (and in solution) in 40% yield following purification by preparative silica thin-layer chromatography (Scheme 1, Figure 2b). Compound **5** was also synthesised⁹⁵ to act as a model for a single bis-pyrrolidine PDI panel and allow comparative studies to the Green Box (Scheme S1.1 and Supporting Information section 1).



Scheme 1. Final procedures in the multi-step synthesis of bis-PDI macrocycle Green Box **4**, and bis-pyrrolidine PDI single panel **5**.

Green Box **4** was fully characterised by ^1H and ^{13}C NMR spectroscopy with full assignment of spectra provided from two-dimensional NMR experiments including COSY, ROESY and HSQC whilst MALDI-TOF and high resolution (ESI) mass spectrometry further confirmed isolation of the desired [1+1] macrocyclic product (Figure 2a and Supporting Information sections 1-3). Cyclic voltammetry of **4** recorded in nitrobenzene revealed two quasireversible oxidation processes ($E^{1/2}_{\text{ox}} = +0.19\text{ V}$; $+0.33\text{ V}$), and no reduction processes within the examined potential window (Figure 2d and Supporting Information section 5). Comparison of the position of these redox couples with those reported in the literature for structurally similar PDI derivatives,^{82,89,90} as well as the single PDI panel reference compound **5** (Table

S5.1, Figure S5.2) indicate these correspond to the sequential oxidations of both PDI units, thus demonstrating the electron-rich nature of the PDI macrocycle.

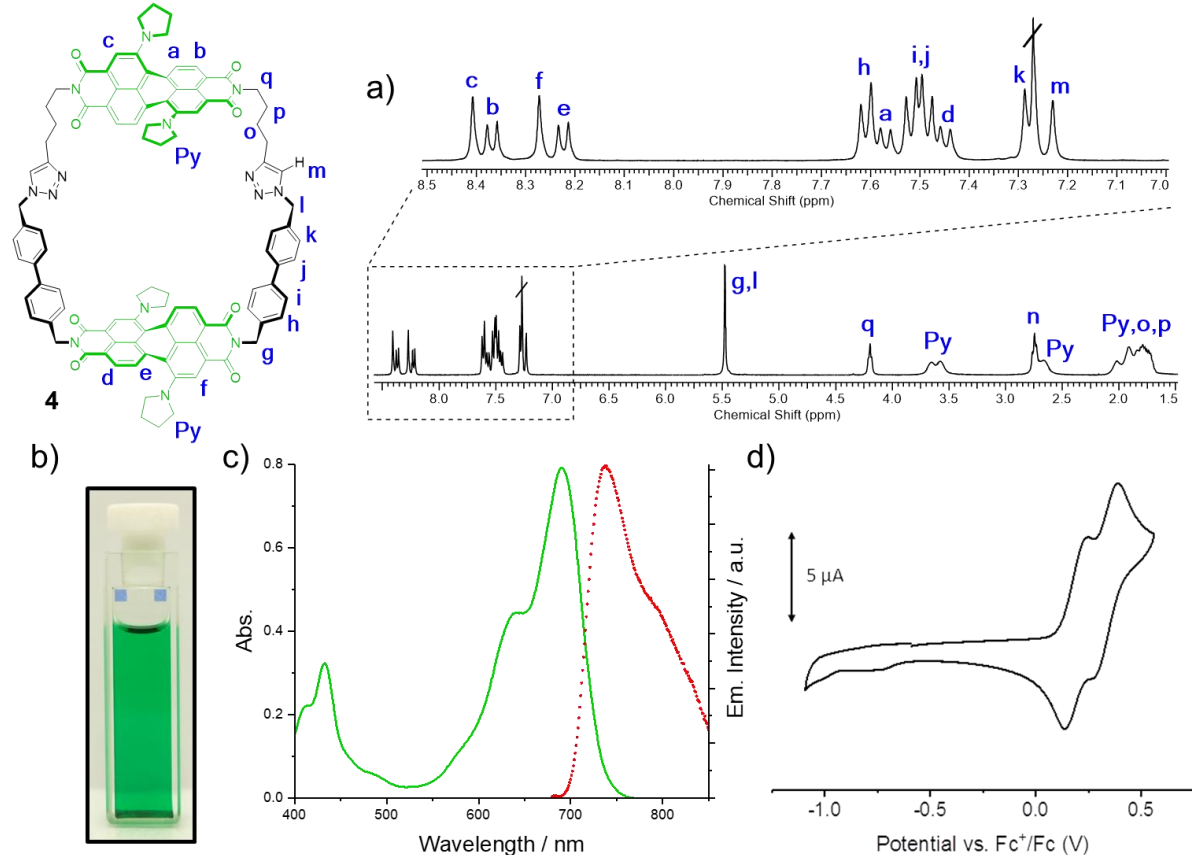


Figure 2. Characterisation of Green Box **4**; (a) ^1H NMR spectrum (CDCl_3 , 298 K, 500 MHz), (b) photograph of a toluene solution (10^{-4} M), (c) electronic absorption (solid line) and fluorescence emission (dotted line) spectra (toluene, 10^{-5} M, $\lambda_{\text{ex}} = 680$ nm) and (d) cyclic voltammogram (nitrobenzene with 0.1 M $[n\text{-Bu}_4\text{N}][\text{BF}_4]$, 0.1 V/s).

Importantly, an absence of broadening of the ^1H NMR spectrum in CDCl_3 up to a maximum concentration of 9 mM indicated that the macrocycle remains monomeric in solution due to the twisted PDI panels (Figure 2a). This was also the case in a number of aromatic organic solvents; electronic absorption and fluorescence emission spectra of the Green Box revealed a well-resolved vibronic fine structure to respective $\text{S}_0 \rightarrow \text{S}_1$ and $\text{S}_1 \rightarrow \text{S}_0$ PDI bands⁹⁶ at $\lambda > 600$ nm (Figure 2c and Supporting Information section 4).^{80,97} Interestingly, the UV-Vis-NIR spectrum of **4** also exhibited solvatochromism (Figure S4.1); with an increase in polarity producing a bathochromic shift in $\lambda_{\text{abs,max}}$ due to the PDI HOMO being localized mainly on the pyrrolidine nitrogen atoms thus giving rise to charge transfer character of the $\text{S}_0 \rightarrow \text{S}_1$ transition.⁶⁰ A significant Stokes shift ($\lambda = 46$ nm) is indicative of the propeller-type contortion of the aromatic framework of the macrocycle bay-substituted PDI motif (Figure 2c).⁴⁹

Fullerene recognition studies

Toluene and o-dichlorobenzene

The solution phase interactions of the Green Box with the two most ubiquitous fullerenes, C_{60} and C_{70} , were investigated by a variety of techniques. Initially these studies were performed in toluene and o-dichlorobenzene (o-DCB) media because these aromatic solvents are known to provide excellent solubilisation of fullerenes.⁹⁸

Photophysical titration experiments were performed in which up to 170 equivalents of fullerene guest were added to a solution of Green Box (host concentration maintained at 10 μM) and monitored by Vis-NIR absorption and fluorescence emission spectroscopies (Figure 3a and Supporting Information section 4).⁹⁹ In all cases the addition of fullerene caused a significant decrease in intensity of the main $\text{S}_0 \rightarrow \text{S}_1$ PDI band ($\lambda_{\text{abs,max}} = 690$ nm in toluene) and the emergence of new absorptions at $\lambda < 615$ nm and $\lambda > 730$ nm (Figures 3a and S4.2 – S4.4). These are diagnostic of new ground state charge transfer aromatic stacking interactions between the tightly associating electron rich macrocyclic host and electron deficient fullerene guest, i.e. formation of complex $[\mathbf{4}]^{\delta+} \rightarrow [\text{C}_{60/70}]^{\delta-}$.^{34,49,56,81,82} Concomitant quenching of the PDI fluorescence emission (up to 29 % ¹⁰⁰) was also observed with C_{60} (Figure 3a), indicative of intermolecular charge transfer between proximal donor and acceptor molecules (vide infra).^{36,49,80,81,101}

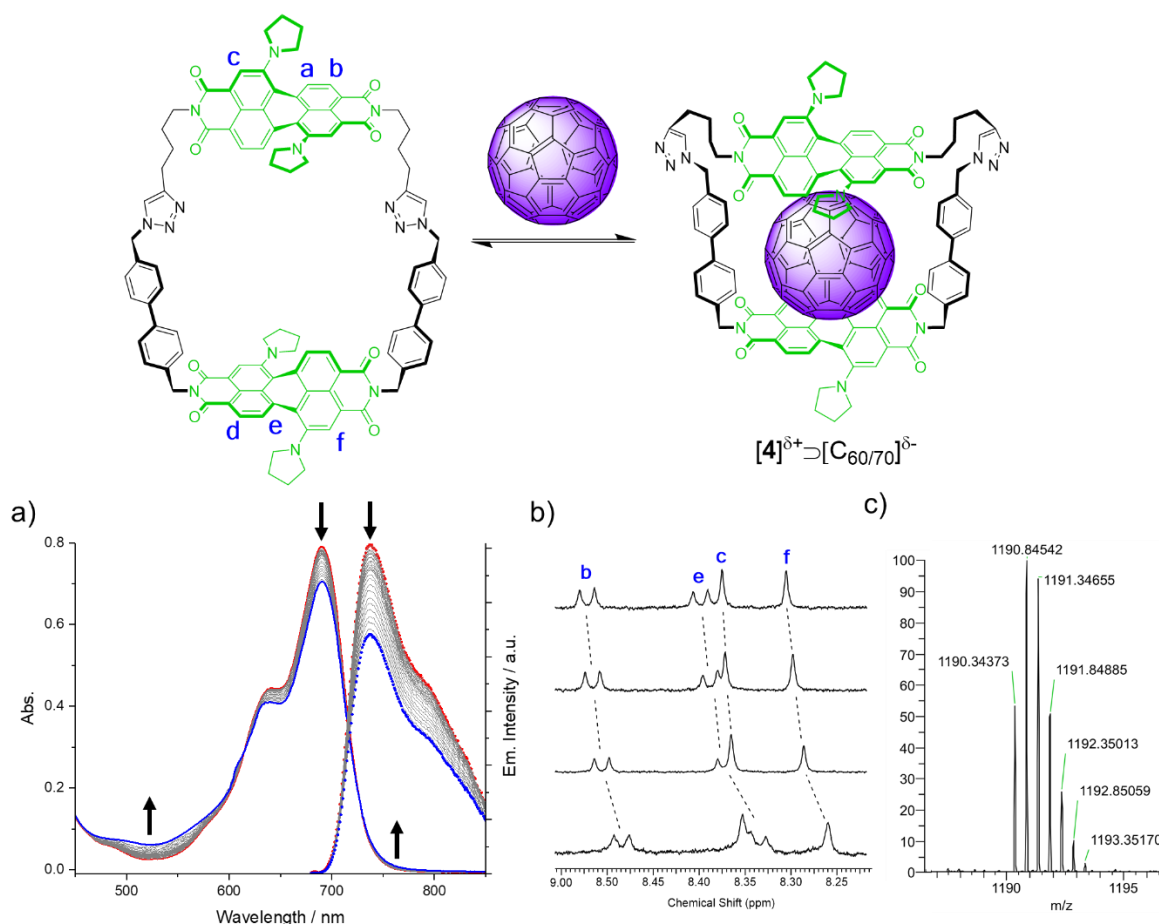


Figure 3. Characterisation of the $[4]^{\delta+}\supset[C_{60}]^{\delta-}$ complex in toluene; (a) electronic absorption (solid line) and fluorescence emission (dotted line) spectra of Green Box upon the titration with C₆₀ (170 eq., toluene, 10^{-5} M, $\lambda_{\text{ex}} = 680$ nm, corrected for C₆₀ absorptions, red line = start point, blue line = end point), (b) ¹H NMR spectroscopic titration of up to three equivalents of C₆₀ into Green Box (d₈ - toluene, [4] = 0.5 mM, 298 K, 500 MHz) and (c) ESI mass spectrum indicating formation of a 1:1 stoichiometric complex ($m/z = [4+C_{60}+2H]^+$).

The formation of several isosbestic points in the Vis-NIR titration spectra ($\lambda_{\text{abs}} = 730, 615, 454$ nm in toluene) indicated the establishment of a thermodynamic equilibrium between host, guest and complex $[4]\supset[C_{60/70}]$ (Figures 3a and S4.2 – S4.4), thereby enabling quantification of fullerene binding in solution (Table 1). Multiwavelength fitting at $\lambda = 690 - 720$ nm, where the largest spectral changes occurred, was performed using Bindfit¹⁰² and revealed 1:2 host:guest stoichiometric binding (Supporting Information section 8).^{103–105} The fullerene association constants are large and comparable to analogous macrocyclic systems containing multiple porphyrin ($K_a = 10^5 \text{ M}^{-1}$)^{44,106} and tetrathiafulvalene ($K_a = 10^6 \text{ M}^{-1}$) units.¹⁰⁷ In all cases K_{a2} is negligible in comparison to K_{a1} , indicating the first and most favourable binding event occurs inside the cavity of the preorganised host such that the fullerene guest is sandwiched between the two PDI units via the formation of strong charge transfer aromatic stacking interactions. The importance of a macrocyclic scaffold to facilitate such cooperativity for fullerene recognition was further highlighted when the single bis-pyrrolidine PDI panel of the Green Box **5** was titrated with C₆₀ in toluene and produced negligible changes to its electronic absorption spectrum (Figure S4.5).¹⁰⁸ Finally, the formation of a strong 1:1 host-guest stoichiometric complex was confirmed by ESI mass spectrometry in which only peaks corresponding to the m/z of the Green Box and a single C₆₀ fullerene species, i.e. $[4]\supset[C_{60}]$, were observed (Figures 3c and S3.2). As expected, collision induced dissociation MS/MS of $[4]\supset[C_{60}]$ triggered ejection of the fullerene guest, generating a peak for the macrocyclic component (Figure S3.3).

In both solvents Green Box exhibits a preference for C₇₀ over C₆₀ which may result from a closer size and shape match with the larger ellipsoidal fullerene as well as enhanced electronic complementarity owing to C₇₀ being more electron deficient.^{36,38,109,110} In agreement with previously reported solution phase fullerene recognition studies, C₆₀ binding is stronger in toluene than o-DCB due to the fact that the latter is a more competitive solvent.^{56,111} However, on moving to the more polar solvent with C₇₀, an enhanced stabilisation of the stronger charge transfer aromatic stacking interactions appears to compensate for this effect.^{112,113}

Table 1. Fullerene association constants (K_{a1} , M^{-1}) for Green Box **4**.^a Determined by Vis-NIR spectroscopy, three expt. mean reported with relative standard deviations < 3%, fitting errors < 5 %, (298 K, λ_{abs} = 690–720 nm, $[4] = 10^{-5}$ M). See Supporting Information section 8.

| | C₆₀ | C₇₀ |
|----------------|-----------------------|-----------------------|
| Toluene | 41,400 | 69,900 |
| o-DCB | 20,300 | 71,700 |

^a 1:2 host:guest binding; for C₆₀ $K_{a2} < 1$, for C₇₀ $K_{a2} \leq 101$.

Proton NMR spectroscopy was employed to understand more about the locus of the fullerene in the Green Box cavity and the nature of the interactions driving their association. The titration of three equivalents of C₆₀ into a d₈-toluene host solution (0.4 mM) produced downfield shifts (up to $\Delta\delta = 0.05$ ppm) of a number of resonances including aromatic PDI based protons, H_{b,c,e,f} (Figures 3b and S2.4). Analogous perturbations of signals were also observed in the more competitive solvent d₄-o-DCB¹¹⁴ (Figure S2.5) and upon titration with C₇₀ (Figure S2.6). Interestingly, the largest downfield shifts occur for proton signals associated with the biphenyl substituted PDI of the Green Box suggesting that the additional aromatic rings and rigid strap offer superior interactions with the fullerene relative to the alkyl-linked half of the cavity. Classical macrocyclic hosts such as cycloparaphenylenes³⁹ and porphyrin-based systems¹¹⁵ have also reported downfield shifts upon complexation with fullerenes. As in the case of Green Box these are ascribed to CH– π ^{116,117} and intimate aromatic stacking interactions with partial charge transfer to the fullerene cage resulting in deshielding of receptor protons. By contrast, a control experiment with the single acyclic bis-pyrrolidine PDI panel **5** exhibited no change to its ¹H NMR spectrum upon titration with C₆₀ (Figure S2.7).

Finally, the existence of ground state electronic communication between fullerene and the Green Box was characterised by electrochemical studies; cyclic voltammograms of macrocycle **4** and $[4] \rightarrow [C_{60}]$ were recorded in o-DCB (Table S5.1). The encapsulation of C₆₀ by the Green Box induced an anodic shift of 20 mV in the first oxidation potential of the bis-pyrrolidine PDI (Figure S5.1), consistent with partial charge transfer between the electron donating macrocycle and electron accepting fullerene and formation of the polarized complex $[4]^{\delta+} \rightarrow [C_{60}]^{\delta-}$.^{34,81,82,101}

Importantly all of the above techniques revealed that full ground state electron transfer to form $[4]^+ \rightarrow [C_{60}]^-$ does not occur in either toluene or o-DCB. However, Green Box PDI fluorescence emission quenching by C₆₀ (Figure 3a) and a HOMO (PDI)–LUMO (C₆₀) gap of 1.25 eV (Table S5.1) indicated that excited state electron transfer processes were energetically favourable over formation of ³C₆₀* (1.50 eV);¹¹⁸ with an estimated free energy change for photoinduced electron transfer from **4** to C₆₀ of $\Delta G_{\text{cs}} = -0.49$ eV (Supporting Information section 9). This motivated further investigation into the excited state behaviour of the Green Box–C₆₀ fullerene complex in toluene,³⁴ using LASER pulses in time resolved EPR spectroscopy (TR-EPR) with CW detection (Figure 4a,b and Supporting Information section 6). Measurements were performed at 85 K, where the low temperature is expected to enhance equilibrium in favour of $[4]^{\delta+} \rightarrow [C_{60}]^{\delta-}$ complex formation. At $\lambda_{\text{ex}} = 600$ nm selected for PDI, the charge separated state $[4]^+ \rightarrow [C_{60}]^-$ is produced (Figure 4a), with both Green Box host and fullerene guest radical ion species clearly resolved, in a peak-to-peak signal width of 6 mT and an absorption-emission (AE) non-Boltzmann, spin polarization pattern. By contrast, in a sample of only PDI macrocycle **4**, a signal width of 50 mT with EEEAAA pattern was observed, characteristic of a molecular triplet state formed via inter-system crossing (Figure 4b). Therefore, in the absence of C₆₀ fullerene acceptor guest, no photoinduced electron transfer processes occur. This represents a rare application of TR-EPR to probe excited state interactions of a supramolecular pristine fullerene complex.

The molecular triplet simulation of PDI macrocycle **4** gives $g = 2.0018$ and zero-field splitting values of $|D| = 723 \pm 5$ MHz and $|E/D|$ at the rhombic limit of 1/3. The lineshape of complex $[4]^+ \rightarrow [C_{60}]^-$ at 85K in a LASER-induced echo detection field sweep (trace i., Figure 4a) exhibits the parallel dipolar splitting of about 22 mT for a modelled average distance of 5.5 Å between PDI and fullerene. The CW-detection of this species further holds a low-intensity signal of molecular triplet of **4**, albeit opposite phase of absorption and emission to **4** alone, Figure 4b. This indicates a different intersystem crossing pathway to the triplet of **4** in presence of C₆₀. There is a more-rapid thermal equilibration in polarization at W-band (94 GHz, Figure 4c, Figure S6.4), consistent with the case of short-lived precursors,¹¹⁹ and the resolution of individual radicals is incomplete at the higher frequency. It is noteworthy that in carotenoid-porphyrin-fullerene triad molecules it is also only a single radical ion that is observed for CW-detection of transient X-band EPR.¹²⁰ Following the method of Maeda, *et al.*, a pulsed ELDOR measurement was used, Figure S6.6, which provides a range of 12–14 MHz for energy separation of the two radicals. This amounts to about 0.4 mT or Δg of ca. 0.0025–0.0029, consistent with difference in g-value of the fullerene anion and PDI macrocycle cation shown in Figure 5d. At W-band, a fit in the limit of two derivative Gaussian lines to the TR-EPR signal provides a separation of 3.5–4.5 mT, matching the expected increase in Zeeman splitting.

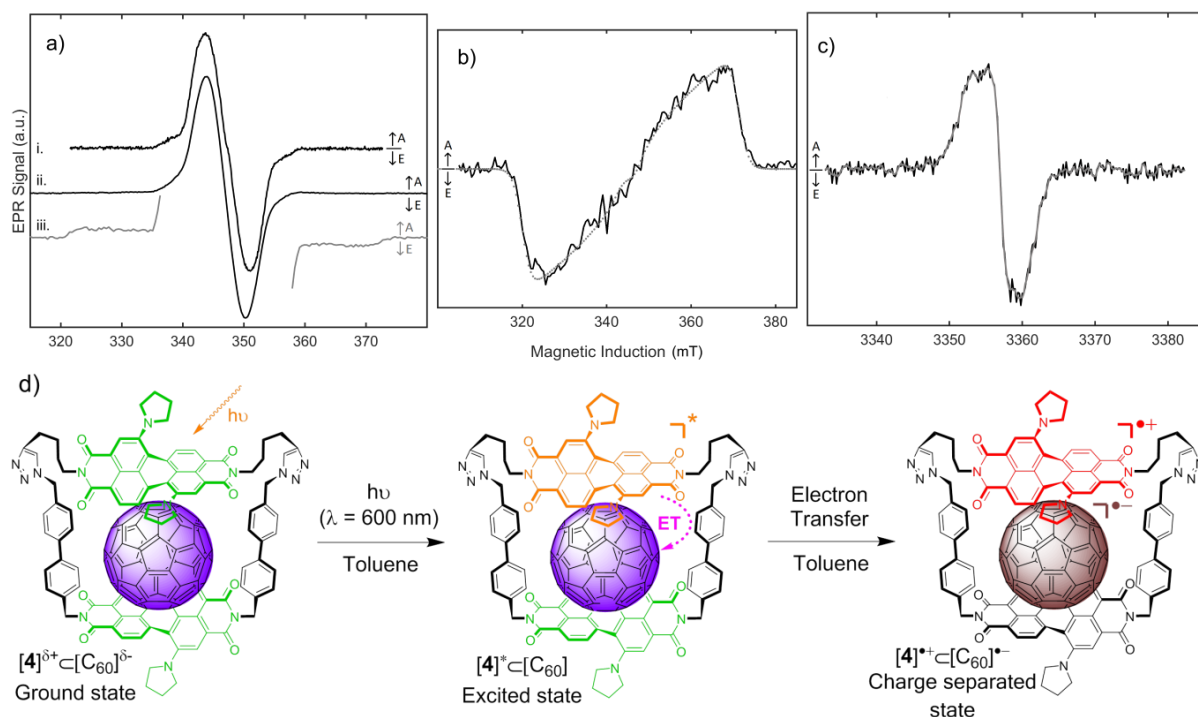


Figure 4. TR-EPR spectra of complex $[4]\supset[C_{60}]$, forming $[4]^{\cdot+}\supset[C_{60}]^{\cdot-}$ upon excitation ($\lambda_{\text{ex}} = 600 \text{ nm}$) at (a) X-band in field-swept echo 16ns- τ -32ns- τ -echo, $\tau=132\text{ns}$ (i.) and CW-detected transient EPR (ii.) with a high-gain acquisition over low-intensity signals (iii.). In panel (b) CW transient EPR is of the host bis-PDI Green Box **4** (100 μM , 85 K, in frozen toluene), black, and triplet state simulation in grey dots, with microwave absorption (A, up arrows) and emission (E, down arrows) indicated in each panel. The microwave frequencies were 9.7281, 9.7262, & 9.7276 GHz in (a) and 9.6898 GHz in (b). Finally, W-band transient CW-detected EPR of $[4]\supset[C_{60}]$ in toluene is shown in (c), with microwave frequency 93.9562 GHz, the grey line is a three-point Savitsky-Golay smooth and (d) a schematic summarising the excited state behaviour of Green Box–fullerene complex $[4]\supset[C_{60}]$ in toluene.

Nitrobenzene

The formation of a supramolecular complex between Green Box and fullerene was also investigated in nitrobenzene because this solvent is significantly more polar than toluene and *o*-DCB ($\epsilon = 35.7$ vs. $\epsilon = 2.4$ and 9.9 respectively) whilst still able to solubilise C_{60} .⁹⁸ The titration of C_{60} into a solution of Green Box in nitrobenzene was monitored by Vis-NIR absorption (Figures 5c and S4.6) and fluorescence emission spectroscopies (Figure S4.7). In this solvent, perturbations to the electronic absorption spectrum were far more drastic than those observed in toluene or *o*-DCB and occurred at guest concentrations two orders of magnitude lower (10 μM vs. 1000 μM), enabling a value of $K_a = 138,000 \text{ M}^{-1}$ to be determined from a 1:1 host–guest stoichiometric model fit (Supporting Information section 8).¹²¹ This association constant is almost an order of magnitude larger than in previous solvents, so that, in agreement with a greater ability to solvate C_{60} ,⁹⁸ their competitive nature increases in the order nitrobenzene \ll toluene $<$ *o*-DCB.

As such, in nitrobenzene, the addition of only a small excess of C_{60} fullerene (purple solution) formed the 1:1 host–guest stoichiometric complex (i.e. mole fraction χ ($[4]\supset[C_{60}]$) = 1) and caused a colour change from green to brown that was visible to the naked eye (Figure 5a). Examination of the resulting fullerene-corrected Vis-NIR spectrum reveals a near 50% decrease in intensity of the main PDI absorption band ($S_0 \rightarrow S_1$ transition, $\lambda_{\text{abs,max}} = 712 \text{ nm}$) with new bands appearing at $\lambda_{\text{abs}} > 800 \text{ nm}$ (Figure 5c) and $\lambda_{\text{abs}} = 542 \text{ nm}$, concomitant with isosbestic points at $\lambda_{\text{abs}} = 582$ and 765 nm (Figures 5c and S4.6). These new absorptions are ascribed to a bis-pyrrolidine PDI radical cation species, $[PDI]^{\cdot+}$,^{122–124} via spectral comparison with an analogous electrochemically generated $[PDI]^{\cdot+}$ species ($\epsilon = 17,300$ vs. $17,400 \text{ M}^{-1} \text{ cm}^{-1}$ at $\lambda_{\text{abs}} = 890 \text{ nm}$).⁸⁹ The stoichiometric oxidation of a single PDI panel of Green Box by C_{60} was also confirmed through the addition of *one* equivalent of the oxidant Cu(II) triflate to macrocycle **4** or bis-pyrrolidine PDI **5**, generating an identical spectrum for $[PDI]^{\cdot+}$ ($\epsilon = 17,000 \text{ M}^{-1} \text{ cm}^{-1}$ at $\lambda_{\text{abs}} = 890 \text{ nm}$, Figure S4.7).¹²⁵ Importantly, relative to the Cu(II) generated spectra, NIR absorptions at $\lambda_{\text{abs}} > 950 \text{ nm}$ were larger for $[4]\supset[C_{60}]$ due to overlapping C_{60} radical anion bands (Figures 5c and S4.7).^{112,126–128} This was clearly demonstrated by the chemical generation of $[C_{60}]^{\cdot-}$ using cobaltocene as the reducing agent (Figure S4.8).^{129,130} Therefore, the NIR spectrum of the complex is the sum of its constituent parts: $[4]^{\cdot+}\supset[C_{60}]^{\cdot-} = [PDI]^{\cdot+} + [C_{60}]^{\cdot-}$ (Figure S4.8).

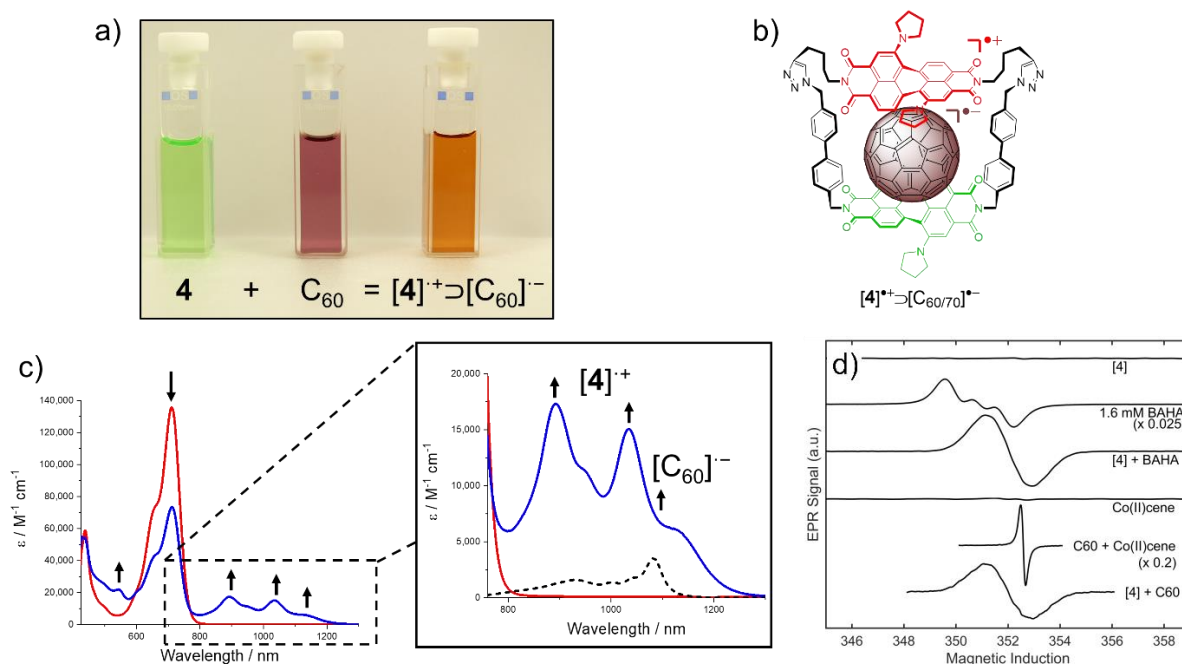


Figure 5. Characterisation of the 1:1 host-guest stoichiometric complex $[4]^{\bullet+}\supset[C_{60}]^{\bullet-}$ in nitrobenzene; (a) Photograph showing naked eye colour change upon mixing of equimolar solutions of Green Box and C_{60} in nitrobenzene (100 μM , $\chi ([4]\supset[C_{60}]) = 1$), (b) structure of the charge separated radical ion paired complex, (c) Vis-NIR electronic absorption spectra of Green Box upon addition of 1.5 equiv. C_{60} (nitrobenzene, 50 μM , $\chi ([4]\supset[C_{60}]) = 1$, Vis-NIR spectra corrected for C_{60} absorptions, red line = host $[4]$, blue line = complex $[4]^{\bullet+}\supset[C_{60}]^{\bullet-}$ where $[4]^{\bullet+} = [\text{PDI}]^{\bullet+}$, for further discussion see Supporting Information section 4). (d) X-band CW-EPR spectra at 100 μM of cation of macrocycle $[4]$ ($[4] + \text{BAHA}$), anion of C_{60} ($C_{60} + \text{cobaltocene}$), and complex of $[4] + C_{60}$. Control spectra were $[4]$ alone, BAHA and cobaltocene at 29 K, $\nu_{\text{mw}} = 9.868 \text{ GHz}$, $P_{\text{mw}} = 2 \text{ mW}$. (EPR in nitrobenzene, except cobaltocene (+ C_{60}) in benzonitrile).

The formation of the radical anion pair was further characterised by electron paramagnetic resonance (EPR) spectroscopy; addition of a small excess of C_{60} into a nitrobenzene solution of Green Box **4** generated a single resonance (g -factor = 2.0029) in nearly stoichiometric amounts (90%) by quantitative EPR. The observed EPR peak-to-peak line width of 1.74 mT contains several unresolved hyperfine features that together with the g -value, closely resemble the chemically-oxidized cation of $[4]$ using oxidant tris(4-bromophenyl)ammoniumyl hexachloroantimonate (BAHA). Chemical reduction of C_{60} with cobaltocene in benzonitrile produced a narrow resonance at $g = 1.9998$, consistent with literature values calculated for chemically and electrochemically generated C_{60} radical anions.^{131–134} While no independent resonance of the C_{60} anion is visible in the solution of $[4] + C_{60}$, it is possible that its inclusion in $[4]^{\bullet+}\supset[C_{60}]^{\bullet-}$ formed in a high dielectric solvent may fundamentally alter the wavefunction and hence g -value of the C_{60} at least in part by sizeable exchange coupling with macrocycle $[4]$. This is supported by the theoretical calculations that indicate significant delocalization of the wavefunction over both the fullerene and macrocycle **4** components (*vide infra*, Figure 9). Limitations of fullerene solubility and sensitivity preclude determination of any splittings in the EPR from exchange coupling. In the frozen solution the lack of g -value resolution is also the case and only a small broaden is observed in Q-band (Figure S6.5). The temperature dependence of the signal amplitudes over 85, 170, & 255 K are consistent with a thermally-isolated spin manifold. Importantly, identical Vis-NIR absorption and EPR spectral changes occurred when mixing of macrocycle **4** and C_{60} was performed under ambient conditions in the absence of light, whilst control experiments using these spectroscopies revealed no radical ion species were present in nitrobenzene solutions of host or guest prior to their combination (Figures S4.13 and S6.1).

Remarkably, these results are all evidence of the occurrence of a thermally promoted, ground state single electron transfer (SET) from the electron rich bis-pyrrolidine PDI donor to an electron deficient C_{60} fullerene cage acceptor upon its tight encapsulation (ultimately as a radical anion) within the Green Box (Figure 5b).^{135,136} Whilst only partial *charge* transfer was observed in toluene and *o*-DCB solvents (*vide supra*, Figure 3), the higher polarity of nitrobenzene facilitates full *ground state electron* transfer and formation of a novel charge separated $[4]^{\bullet+}\supset[C_{60}]^{\bullet-}$ complex. Importantly, ground state SET to C_{60} is extremely rare, with examples limited to simple secondary and tertiary amine donors^{128,137,138} such as 1,3-diaminepropane¹²⁷ or with endohedral metallofullerene (EMF) acceptors that exhibit more favourable reduction potentials than their empty cage analogues.^{135,138} Indeed, to the best of our knowledge, the Green Box is the first rationally designed synthetic receptor capable of recognising and sensing a pristine fullerene via

thermally promoted SET from host to guest, with previous systems reporting only partial charge transfer in the ground state.^{33,34,47,49,54,56,139–141}

SET occurs under ambient conditions; i.e. at room temperature, in oxygenated solvent and is unaffected by natural light (i.e. not a photoinduced process). The robustness of this process was also demonstrated when analogous Vis-NIR spectral changes were observed with C₇₀ (Figure S4.13) and with C₆₀ under more dilute conditions (1 μM host solution, Figure S4.6). As expected, the formation of new radical ion species in solution results in an almost complete quenching of Green Box PDI excited state fluorescence emission (90 % ¹⁰⁰) upon addition of fullerene (Figure S4.12).⁸⁰ Further evidence for the formation of [4]^{•+}⊃[C₆₀]^{•-} radicals was provided by significant broadening of resonances, predominantly PDI protons (H_{b,c,e,f}), in the ¹H NMR spectrum (Figure S2.8).

The formation of isosbestic points in the Vis-NIR spectra (Figures 5c and S4.6) indicate the formation of a thermodynamic equilibrium between the ‘neutral’ and charge separated radical ion paired complexes, [4]^{δ+}⊃[C₆₀]^{δ-} and [4]^{•+}⊃[C₆₀]^{•-} respectively. To investigate whether SET between Green Box and C₆₀ fullerene is a truly reversible process, the Vis-NIR electronic absorption spectrum of the 1:1 host–guest stoichiometric complex [4]⊃[C₆₀] was measured in nitrobenzene:toluene solvent mixtures (Figure 6). Increasing the proportion of the less polar solvent (toluene) caused a decrease in intensity of NIR radical ion peaks (λ_{abs} = 890, 945, 1035 nm) concomitant with an increase in the main PDI absorption band (λ_{abs,max} = 712 nm), confirming thermodynamic equilibrium (isosbestic point λ = 762 nm) and a clear solvatochromism to the charge separated state.¹³⁵ Decreasing the temperature of the solution had the same effect (isosbestic point λ = 763 nm, Figure S4.11). As expected from solvent competitiveness, guest binding was weaker in the mixed solvent system than in neat nitrobenzene (K_{a1} = 53,100 M⁻¹ in 1:1 v/v nitrobenzene:toluene, Supporting Information section 8).

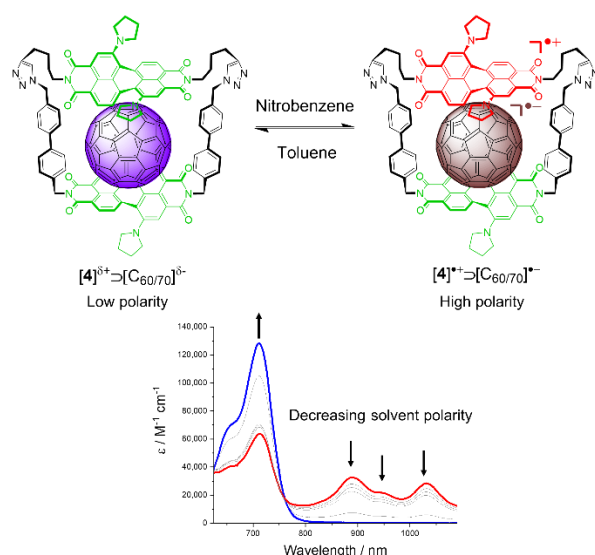


Figure 6. Vis-NIR electronic absorption spectra of the 1:1 host–guest stoichiometric complex [4]⊃[C₆₀] measured in v/v nitrobenzene:toluene solvent mixtures of decreasing polarity (red line = 9:1 v/v nitrobenzene:toluene, grey line = intermediate v/v ratios, blue line = 1:9 v/v nitrobenzene:toluene).

In comparison to o-DCB, the host and guest redox potentials recorded in nitrobenzene indicate electron transfer is more thermodynamically favourable (Table S5.1) and,¹⁴² as shown experimentally, occurs in this solvent. Furthermore, the extremely strong association (K_a = 138,000 M⁻¹) between macrocyclic host and fullerene guest (i.e. formation of [4]⊃[C₆₀], see Supporting Information section 9b) helps promote a spontaneous redox process.^{112,143} Previous studies have also reported ground state electron transfer from electron rich azacrown¹³⁸ or thiacrown ether¹⁴³ macrocyclic donors to tightly bound fullerene guests. This is further supported by the observation that titration of the single bis-pyrrolidine PDI panel **5** with a large excess of C₆₀ resulted in negligible radical formation (Figure S4.17).

EPR spectroscopy revealed that C₆₀^{•-} was persistent in a solution of complex [4]^{•+}⊃[C₆₀]^{•-} in nitrobenzene on the benchtop under ambient conditions for several days (Figure S6.2), albeit with a lower signal intensity than at the start. The durability of this radical ion in solution prompted a kinetic study by Vis-NIR absorption and EPR spectroscopies. A time course measurement of the electronic absorption band associated with [PDI]^{•+} at λ_{abs} = 890 nm gave a PDI radical cation half-life of t_{1/2} > 600 minutes (Figure S7.1).^{136,144–146} The time dependence of the EPR spectrum revealed similar kinetic behaviour (Figures S6.3, S7.2). It has been shown that sterically hindered tertiary amines,¹⁴⁵ such as those present in the bis-pyrrolidine PDI panels of **4**, produce a more persistent spin density in solution than secondary or less bulky amines^{128,138,145} for which new covalent bond forming reaction pathways can compete.¹⁴⁷

After three days on the bench, ^1H and ^{13}C NMR spectroscopy, mass spectrometry and TLC analysis indicated partial regeneration of neutral Green Box and C_{60} fullerene species due to back electron transfer (Figure S4.15-4.16).^{144,145,148} Molecular oxygen can facilitate charge recombination,¹²⁸ however, little change to kinetic behaviour was found when experiments were repeated under an atmosphere of nitrogen (Figures S7.3). Instead, analysis of solutions of the $[\mathbf{4}]^+\supset[\text{C}_{60}]^-$ complex and C_{60} alone by dynamic light scattering over this time scale revealed the gradual formation of fullerene aggregates in nitrobenzene (Figure S7.4), and so a probable cause for slow radical recombination.^{149,150} Relative to toluene and o-DCB, this solvent is known to provide poorer solubility.⁹⁸ However, re-dispersion of C_{60} fullerene by sonication of the sample acted to regenerate the radical pair, as did the addition of further free guest (Figures S7.5 and S7.6). There was no time dependence to the spectral changes arising from charge transfer interactions in toluene solution, signifying the resilience of the polarised complex $[\mathbf{4}]^{\delta+}\supset[\text{C}_{60}]^{\delta-}$ (Figure S7.7) in this solvent. Therefore, the contrasting electronic behaviour of the Green Box receptor serves to highlight the importance of solvent on not only dictating the thermodynamics (partial *charge* transfer vs. full *electron* transfer) but also the kinetics (stability of each complex type) involved in the non-covalent recognition of fullerenes.

Molecular Modelling studies

Further structural insights into the host-guest complex between macrocycle **4** and C_{60} were obtained by molecular modelling. A stochastic conformational search, carried out by Molecular Dynamics simulations (Supporting Information section 10), showed that the flexible Green Box can encapsulate the C_{60} guest in different conformational shapes. Two distinct binding scenarios, **A** and **B**, were selected and investigated by Density Functional Theory (DFT). These calculations were carried out with Gaussian09,¹⁵¹ at the $\omega\text{B97XD}/6\text{-}31\text{G(d)}$ level, in gas-phase and in implicit models of toluene or nitrobenzene, through the SMD variation of IEFPCM.¹⁵² Moreover, in agreement with the experimental findings, these structures were initially optimized in the ground state as singlets.

The **A** and **B** alternative scenarios of $[\mathbf{4}]\supset[\text{C}_{60}]$ are illustrated in Figure 7 with the DFT optimized structures in toluene, while Figure S10.1 displays the computed structures in nitrobenzene. The overlap between structures optimized in gas-phase and in solvent models, yielded low RSMD values from 0.07 to 0.42 Å (Table S10.1), indicating that the computed structures are similar regardless of the optimization media. Structural analysis was therefore focused on the structures optimized in toluene.

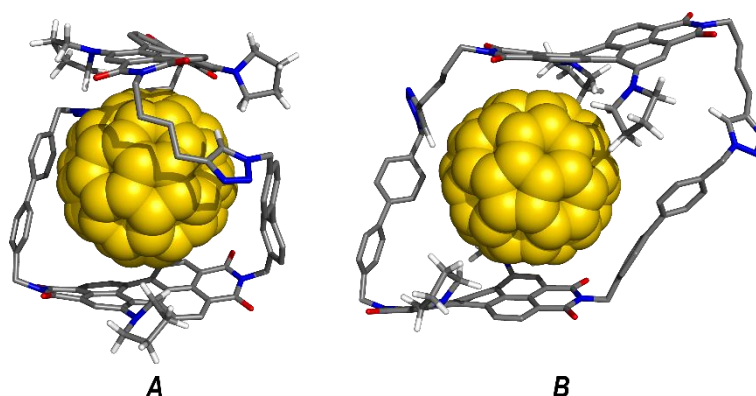


Figure 7. DFT structures of $[\mathbf{4}]\supset[\text{C}_{60}]$ of binding arrangements **A** and **B** optimised in toluene for the singlet state. The C_{60} guest is shown in spheres and the macrocyclic host is shown in sticks, with the C–H protons hidden for clarity, except those in the triazole and pyrrolidine moieties.

In **A**, the Green Box macrocycle wraps the C_{60} guest in an helicoidal fashion, with the PDI moieties twisted by *ca.* 70°, as given by the average values of dihedral angle θ (Scheme S10.1 and Table S10.2). Moreover, both PDI fragments display concave surfaces, with depths of 0.40 and 0.32 Å measured from the centroid of the central six-membered ring ($\text{C}_{6,\text{host}}$) to the plane defined by the carbon atoms of the four carbonyl groups of the top and bottom PDI units, as identified in Scheme S10.1. These values indicate that the PDI units provide adaptable surfaces to accommodate the fullerene guest. Furthermore, the closest rings of C_{60} facing the PDI panels are 3.44 and 3.59 Å between their centroids and the plane of the central six-membered ring (PDI_{C_6} plane) in the top and bottom PDI units, respectively ($\text{C}_{60}\cdots\text{PDI}_{\text{C}_6}$ distance). These intermolecular distances are consistent with the existence of π – π aromatic stacking interactions between the convex C_{60} host and the concave surfaces of the PDI units.^{153–155} In agreement with NMR data, the spatial disposition of the pyrrolidine substituents allow several C–H protons to establish C–H $\cdots\pi$ interactions with C_{60} , with C–H $_{\text{pyr}}\cdots\text{C}_{60}$ distances ranging from 2.56 to 3.36 Å (Table S10.2).

In contrast with **A**, in the computed binding scenario **B**, the macrocycle presents a “rhombic” shape with the two PDI panels adopting an approximately parallel disposition (Figure 7B and Table S10.2). Noteworthy, C_{60} interacts with half of the surface of each PDI moiety, a benzo[*de*]isoquinoline-dione fragment (PDI_{half} plane). Indeed, the two PDI units facing the fullerene guest are now convex, with depths of -0.7 and -0.4 Å in the top and bottom PDI panels, respectively. The C_{60} rings closest to the planar benzo[*de*]isoquinoline-dione fragments present $C_{60}\cdots\text{PDI}_{\text{half}}$ distances of 3.43 (top) and 3.60 Å (bottom), also indicating the occurrence of π - π interactions. This binding arrangement is also stabilized by a few short C-H $\cdots\pi$ contacts between the pyrrolidine substituents and the C_{60} guest, with C-H_{pyr} $\cdots C_{60}$ distances varying between 2.67 and 3.03 Å.

The interaction energies in arrangements **A** and **B** were calculated as $\Delta E_{\text{int}} = E_{[4]\supset[C_{60}]} - (E_4 + E_{C_{60}}) + BSSE$, where $E_{[4]\supset[C_{60}]}$ is the total energy of the host-guest complex, E_4 and $E_{C_{60}}$ are the energies of the host and guest partners in the geometries found in the optimized complex, and $BSSE$ is the basis set superposition error determined from gas-phase optimized structures of $[4]\supset[C_{60}]$.^{156,157} These indicate that in arrangement **A** the macrocycle is more tightly bonded to the fullerene guest, being preferred by 5.4 and 5.7 kcal mol⁻¹ in toluene and in nitrobenzene, in this order. Interestingly, the total energies of the host-guest complex find binding arrangement **B** is favoured by 7.2 and 8.6 kcal mol⁻¹, for toluene and nitrobenzene, respectively.¹⁵⁸ This shows that the structural change of **4** from a lower energy conformation in solution to a helicoidal shape upon C_{60} encapsulation (**A**) has a larger energy penalty to overcome.¹⁵⁹

In the distribution of Natural Population Analysis charges of both binding arrangements in both solvents, **4** has a slight positive net charge (+0.02 *e*), while C_{60} has a symmetric negative charge, consistent with the experimental evidence for polarization of the host-guest complex ($[4]^{\delta+}\supset[C_{60}]^{\delta-}$). As expected from electrochemical studies, the HOMO is PDI macrocycle-based whilst the LUMO is primarily concentrated on the C_{60} fullerene guest. Frontier orbitals are depicted in Figure 8 for **A** and **B** in toluene and are equivalent to those in nitrobenzene (Figure S10.2). These calculations also indicate a subtle difference between binding scenarios; in **A** the HOMO is mainly located on the aryl substituted PDI (bottom), with the HOMO-1 assigned to the other PDI panel (top), whilst in binding arrangement **B**, these orbitals occupy the opposite PDI panels. The energies of these frontier orbitals are summarized in Table S10.3. In further agreement with experimental results, the HOMO-LUMO energy gap is smaller in nitrobenzene *vs.* toluene, with the LUMO in fact being more accessible in **B** than **A**, for facilitating electronic transitions from the ground state to this orbital.

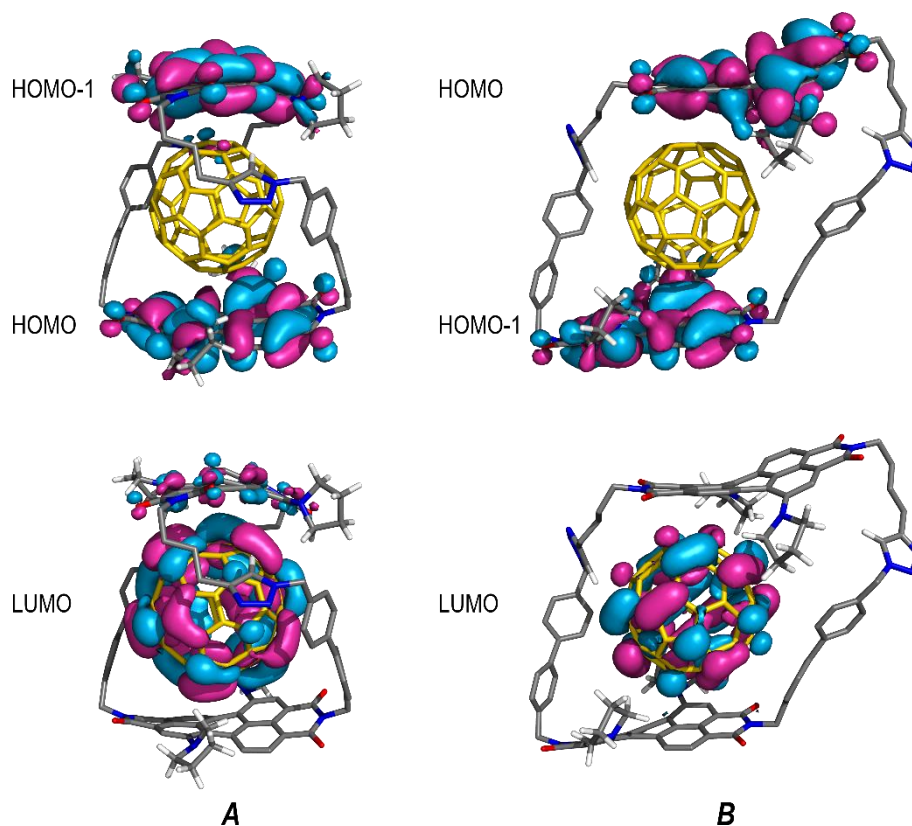


Figure 8. Isodensity surface plots of frontier molecular orbitals HOMO-1, HOMO and LUMO of $[4]\supset[C_{60}]$ in binding arrangements **A** and **B**, for the singlet state optimized structures in toluene (density value of $\pm 0.015 \text{ e a}_0^{-3}$).

Following experimental evidence for the existence of the Green Box- C_{60} complex as a ground state di-radical in nitrobenzene, the **A** and **B** binding arrangements were re-optimized in the triplet state. The DFT optimized structures are illustrated in Figure S10.3 and are identical to their corresponding singlets, with RMSD values of 0.27 (**A**) and 0.07 Å (**B**). Noteworthy, these alternative binding arrangements have different Mulliken spin density distributions, as summarized in Table S10.3 and shown in Figure 9. While in **A** the spin density is concentrated only on the alkyl substituted PDI panel (top), in **B** it is divided over this PDI moiety and C_{60} , with a total density of 1 for the host and for the guest, leading to a charge distribution consistent with transference of one electron from **4** to C_{60} , *i.e.*, the formation of the radical ion pair $[4]^+ \supset [C_{60}]^-$ (Figure 5). The larger contributions for the PDI panel spin density are from the pyrrolidine nitrogen atoms (Table S10.3). In **B**, the unpaired electrons are found in the α -HOMO comprising the C_{60} (LUMO in the singlet state) and in α -HOMO-2 enclosing the top PDI panel (HOMO-1 in the singlet state). Overall, taking **A** and **B** together, significant delocalization of the triplet wavefunction is apparent and consistent with the EPR analysis (*vide supra*).

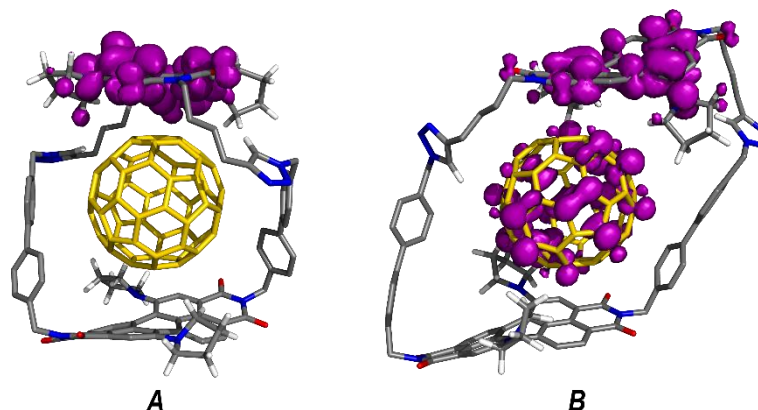


Figure 9. Triplet spin density plots of $[4] \supset [C_{60}]$ in binding arrangements **A** and **B**, for the structures optimized in nitrobenzene (density value of 0.001 e a_0^{-3}).

Conclusions

This work describes the rational design, synthesis and in-depth $C_{60/70}$ fullerene recognition investigation of a novel macrocycle which, due to the two bis-bay substituted pyrrolidine–perylene diimide-based panels, is nicknamed the “Green Box” **4**. Aryl and alkyl spacer units that separate the two twisted aromatic PDI surfaces act to create a rigid yet size-adaptable, electron rich cavity capable of encapsulating electron deficient fullerene guests such as C_{60} or C_{70} to form a supramolecular complex, $[4] \supset [C_{60/70}]$. Importantly, strong solution phase fullerene recognition (micromolar affinity) was shown to occur within this macrocyclic receptor framework and not to an acyclic single PDI panel **5**. Characterisation of the complex and the fundamental non-covalent interactions that drive its formation were elucidated through a variety of techniques including electronic absorption, fluorescence emission, NMR and EPR spectroscopies, electrochemistry and mass spectrometry and DFT calculations.

The electronic complementarity between Green Box PDI receptor and fullerene guest was manifested in ground state partial charge transfer in toluene and o-DCB solution ($[4]^{\delta+} \supset [C_{60/70}]^{\delta-}$), with such chromogenic interactions in part responsible for an enhancement in binding of the more electron deficient C_{70} over C_{60} . To the best of our knowledge, this is the first report of intermolecular electronic communication in the ground state between perylene diimide and fullerene. Therefore, alongside more renowned aromatic derivatives such as porphyrin,^{44,141} cycloparaphenylene^{39,160} and tetrathiafulvalene,^{107,161} twisted electron rich PDIs are introduced as new motifs for fullerene recognition.

Whilst time resolved EPR spectroscopy revealed that complete single electron transfer (SET) between Green Box donor and fullerene acceptor only occurred via an excited state in toluene, switching the solvent to nitrobenzene stimulated intermolecular *ground state* SET without the need for photoirradiation under ambient conditions.^{128,136} Facilitated by an exceptionally strong association between donor and acceptor, thermally-allowed SET within a supramolecular host–fullerene guest complex is unprecedented behaviour unique to the Green Box host. Noteworthy, formation of the di-radical ion-pair complex $[4]^+ \supset [C_{60}]^-$ was supported by DFT calculations. The components were characterised by Vis-NIR electronic absorption and EPR spectroscopies, and shown to be remarkably bench-stable with signals still present in solution after several days. Importantly, temperature, and a dependence on solvent permittivity revealed the charge-separated state complex $[4]^+ \supset [C_{60}]^-$ to exist in thermal equilibrium with its polarised analogue $[4]^{\delta+} \supset [C_{60}]^{\delta-}$. Such reversible electron transfer processes play a key role in biological energy conversion.¹⁸ The above provides a rare example of an artificial supramolecular donor-acceptor ensemble¹³⁶ in which a solvent stimulus is used to switch

between two extremes of the energy continuum,⁵⁷ to promote either charge separation or recombination, in similar fashion to cofactors found in natural systems.^{162–164}

In summary, Green Box permits intermolecular, tuneable partial charge or full electron transfer in the ground state to pristine fullerenes, the former being unprecedented with perylene diimides and the latter unknown in a synthetic fullerene-based dyad system (Figure 10). This generates a biomimetic supramolecular ensemble that undergoes reversible electron transfer processes. Further investigation into the applications of this unique PDI donor-fullerene acceptor behaviour within molecular organic electronics and optical carbon nanomaterials or functional devices, including new routes to fullerene purification, are currently ongoing.

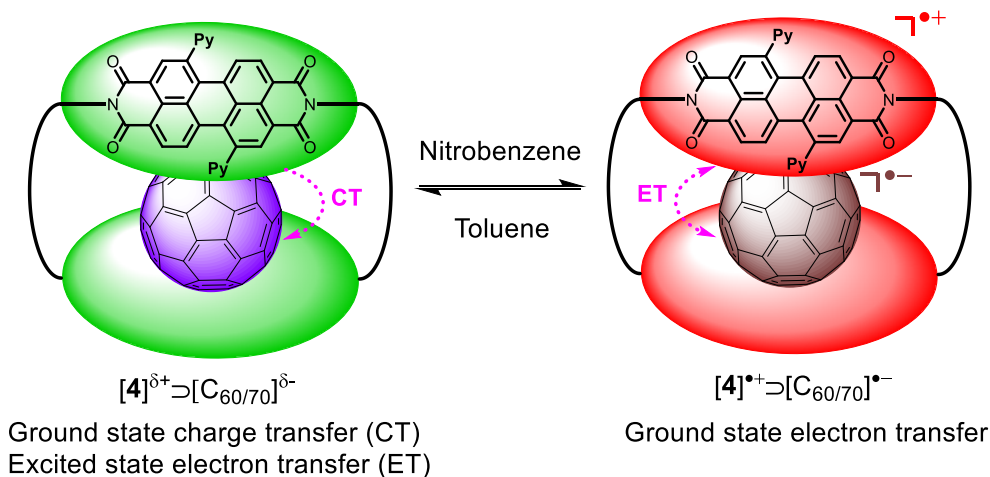


Figure 10. Schematic showing the solvent tuneable ground and excited state electronic interactions of the Green Box host [4] donor–fullerene guest acceptor supramolecular complex ensemble. (Py = pyrrolidine).

Associated Content

Further details of synthetic procedures, characterization, electrochemical and spectroscopic data, molecular modeling methods and additional discussion including Schemes, Figures and Tables are included in the Supporting Information (Sections 1-10). Tables S10.4 – S10.6 are available separately for download.

Author Information

Corresponding Authors

*timothy.barendt@chem.ox.ac.uk

*paul.beer@chem.ox.ac.uk

ORCID:

Timothy A. Barendt: 0000-0002-9806-4381

Maria A. Lebedeva: 0000-0002-3543-6416

William K. Myers: 0000-0001-5935-9112

Paul D. Beer: 0000-0003-0810-9716

Igor Marques: 0000-0003-4971-9932

Vítor Félix: 0000-0001-9380-0418

Acknowledgements

T.A.B. thanks Christ Church and the John Fell Fund (162/013), University of Oxford for funding. W.K.M. is supported by UK EPSRC (EP/L011972/1), grant to Centre for Advanced ESR, CAESR. The theoretical studies were supported

by projects PTDC/QEQ-SUP/4283/2014 and CICECO – Aveiro Institute of Materials (UID/CTM/50011/2019), financed by National Funds through the FCT/MEC and co-financed by QREN-FEDER through COMPETE under the PT2020 Partnership Agreement. I.M. is grateful for a postdoctoral grant (BPD/UI98/6065/2018) under project “pAGE” (Centro-01-0145-FEDER-000003), co-funded by Centro 2020 programme, Portugal 2020, European Union, through the European Regional Development Fund.

References

- (1) Langa, F.; Nierengarten, J.-F. *Fullerenes: Principles and Applications*; Royal Society of Chemistry, Royal Society of Chemistry: Cambridge, UK, 2007.
- (2) Delgado, J. L.; Herranz, M. Á.; Martín, N. The Nano-Forms of Carbon. *J. Mater. Chem.* **2008**, *18* (13), 1417–1426. <https://doi.org/10.1039/B717218D>.
- (3) Collavini, S.; Delgado, J. L. Fullerenes: The Stars of Photovoltaics. *Sustain. Energy Fuels* **2018**, *2* (11), 2480–2493. <https://doi.org/10.1039/C8SE00254A>.
- (4) Delgado, J. L.; Bouit, P.-A.; Filippone, S.; Herranz, M. Á.; Martín, N. Organic Photovoltaics: A Chemical Approach. *Chem. Commun.* **2010**, *46* (27), 4853–4865. <https://doi.org/10.1039/C003088K>.
- (5) Castro, E.; Murillo, J.; Fernandez-Delgado, O.; Echegoyen, L. Progress in Fullerene-Based Hybrid Perovskite Solar Cells. *J. Mater. Chem. C* **2018**, *6* (11), 2635–2651. <https://doi.org/10.1039/C7TC04302C>.
- (6) Grant, P. Superconductivity: Up on the C₆₀ Elevator. *Nature* **2001**, *413* (6853), 264–265. <https://doi.org/10.1038/35095149>.
- (7) Dagotto, E. The Race to Beat the Cuprates. *Science* **2001**, *293* (5539), 2410–2411. <https://doi.org/10.1126/science.1065711>.
- (8) Iwasa, Y. Superconductivity: Revelations of the Fullerenes. *Nature* **2010**, *466* (7303), 191–192. <https://doi.org/10.1038/466191a>.
- (9) Rašović, I. Water-Soluble Fullerenes for Medical Applications. *Mater. Sci. Technol.* **2016**, 1–18. <https://doi.org/10.1080/02670836.2016.1198114>.
- (10) Rašović, I.; Porfyrakis, K. Functionalisation of Fullerenes for Biomedical Applications. In *Reference Module in Materials Science and Materials Engineering*; Elsevier, 2018. <https://doi.org/10.1016/B978-0-12-803581-8.11224-X>.
- (11) Nakamura, E.; Isobe, H. Functionalized Fullerenes in Water. The First 10 Years of Their Chemistry, Biology, and Nanoscience. *Acc. Chem. Res.* **2003**, *36* (11), 807–815. <https://doi.org/10.1021/ar030027y>.
- (12) Guldi, D. M.; Illescas, B. M.; Atienza, C. M.; Wielopolski, M.; Martín, N. Fullerene for Organic Electronics. *Chem. Soc. Rev.* **2009**, *38* (6), 1587–1597. <https://doi.org/10.1039/B900402P>.
- (13) Martín, N.; Sánchez, L.; Herranz, M. Á.; Illescas, B.; Guldi, D. M. Electronic Communication in Tetrathiafulvalene (TTF)/C₆₀ Systems: Toward Molecular Solar Energy Conversion Materials? *Acc. Chem. Res.* **2007**, *40* (10), 1015–1024. <https://doi.org/10.1021/ar700026t>.
- (14) Lebedeva, M. A.; Chamberlain, T. W.; Khlobystov, A. N. Harnessing the Synergistic and Complementary Properties of Fullerene and Transition-Metal Compounds for Nanomaterial Applications. *Chem. Rev.* **2015**, *115* (20), 11301–11351. <https://doi.org/10.1021/acs.chemrev.5b00005>.
- (15) D’Souza, F.; Ito, O. Supramolecular Donor–Acceptor Hybrids of Porphyrins/Phthalocyanines with Fullerenes/Carbon Nanotubes: Electron Transfer, Sensing, Switching, and Catalytic Applications. *Chem. Commun.* **2009**, *0* (33), 4913–4928. <https://doi.org/10.1039/B905753F>.
- (16) Echegoyen, L.; Echegoyen, L. E. Electrochemistry of Fullerenes and Their Derivatives. *Acc. Chem. Res.* **1998**, *31* (9), 593–601. <https://doi.org/10.1021/ar970138v>.
- (17) Hiroshi, I.; Kiyoshi, H.; Tsuyoshi, A.; Masanori, A.; Seiji, T.; Tadashi, O.; Masahiro, S.; Yoshiteru, S. The Small Reorganization Energy of C₆₀ in Electron Transfer. *Chem. Phys. Lett.* **1996**, *263* (3), 545–550. [https://doi.org/10.1016/S0009-2614\(96\)01244-4](https://doi.org/10.1016/S0009-2614(96)01244-4).
- (18) *The Photosynthetic Reaction Center*; Deisenhofer, J., Norris, J. R., Eds.; Academic Press: San Diego, CA, **1993**. <https://doi.org/10.1016/C2009-0-02600-2>.
- (19) Campidelli, S.; Mateo-Alonso, A.; Prato, M. Chapter 7: Fullerenes for Material Science. In *Fullerenes*; 2007; pp 191–220. <https://doi.org/10.1039/9781847557711-00191>.
- (20) Guldi, D. M. Fullerene–Porphyrin Architectures; Photosynthetic Antenna and Reaction Center Models. *Chem. Soc. Rev.* **2002**, *31* (1), 22–36. <https://doi.org/10.1039/B106962B>.
- (21) Guldi, D. M.; Giacalone, F.; Torre, G. de la; Segura, J. L.; Martín, N. Topological Effects of a Rigid Chiral Spacer on the Electronic Interactions in Donor–Acceptor Ensembles. *Chem. – Eur. J.* **2005**, *11* (24), 7199–7210. <https://doi.org/10.1002/chem.200500209>.
- (22) Hudhomme, P.; Williams, R. M. Energy and Electron Transfer in Photo- and Electro-Active Fullerene Dyads. In *Handbook of Carbon Nano Materials; World Scientific Series on Carbon Nanoscience*; WORLD SCIENTIFIC, **2011**; Vol. Volume 1 & 2, pp 545–591. https://doi.org/10.1142/9789814327824_0017.
- (23) Barendt, T. A.; Rašović, I.; Lebedeva, M. A.; Farrow, G. A.; Auty, A.; Chekulaev, D.; Sazanovich, I. V.; Weinstein, J. A.; Porfyrakis, K.; Beer, P. D. Anion-Mediated Photophysical Behavior in a C₆₀ Fullerene [3]Rotaxane Shuttle. *J. Am. Chem. Soc.* **2018**, *140* (5), 1924–1936. <https://doi.org/10.1021/jacs.7b12819>.

- (24) Kirner, S. V.; Henkel, C.; Guldi, D. M.; Jr, J. D. M.; Schuster, D. I. Multistep Energy and Electron Transfer Processes in Novel Rotaxane Donor–Acceptor Hybrids Generating Microsecond-Lived Charge Separated States. *Chem. Sci.* **2015**, *6* (12), 7293–7304. <https://doi.org/10.1039/C5SC02895G>.
- (25) Mateo-Alonso, A. Mechanically Interlocked Molecular Architectures Functionalised with Fullerenes. *Chem. Commun.* **2010**, *46* (48), 9089–9099. <https://doi.org/10.1039/C0CC03724A>.
- (26) Mateo-alonso, A. Fullerene-Containing Rotaxanes and Catenanes. In *Supramolecular Chemistry of Fullerenes and Carbon Nanotubes*; Nazariortín, Nierengarten, J.-F., Eds.; Wiley-VCH Verlag GmbH & Co. KGaA, **2012**; pp 107–126.
- (27) Megiatto, Jr., J. D.; Schuster, D. I. Chapter 10. Interlocked Artificial Photosynthetic Model Systems Composed of Electron-Donor and C₆₀ Fullerene Units. In *RSC Nanoscience & Nanotechnology*; Langa De La Puente, F., Nierengarten, J.-F., Eds.; Royal Society of Chemistry: Cambridge, UK, **2011**; pp 354–385.
- (28) Mateo-Alonso, A.; Ehli, C.; Rahman, G. M. A.; Guldi, D. M.; Fioravanti, G.; Marcaccio, M.; Paolucci, F.; Prato, M. Tuning Electron Transfer through Translational Motion in Molecular Shuttles. *Angew. Chem. Int. Ed.* **2007**, *46* (19), 3521–3525. <https://doi.org/10.1002/anie.200605039>.
- (29) Guldi, D. M.; Ramey, J.; Martínez-Díaz, M. V.; Escosura, A. de la; Torres, T.; Ros, T. D.; Prato, M. Reversible Zinc Phthalocyanine Fullerene Ensembles. *Chem. Commun.* **2002**, *0* (23), 2774–2775. <https://doi.org/10.1039/B208516J>.
- (30) Segura, M.; Sánchez, L.; de Mendoza, J.; Martín, N.; Guldi, D. M. Hydrogen Bonding Interfaces in Fullerene•TTF Ensembles. *J. Am. Chem. Soc.* **2003**, *125* (49), 15093–15100. <https://doi.org/10.1021/ja036358n>.
- (31) Herranz, M. Á.; Giacalone, F.; Sánchez, L.; Martín, N. Chapter 6:Hydrogen Bonding Donor–Acceptor Carbon Nanostructures. In *Fullerenes: Principles and Applications*; Royal Society of Chemistry: Cambridge, UK, **2007**; pp 152–190. <https://doi.org/10.1039/9781847557711-00152>.
- (32) Electron transfer in a non-covalent donor–acceptor network is as efficient as that in a covalent system.³¹
- (33) Rizzuto, F. J.; Wood, D. M.; Ronson, T. K.; Nitschke, J. R. Tuning the Redox Properties of Fullerene Clusters within a Metal–Organic Capsule. *J. Am. Chem. Soc.* **2017**, *139* (32), 11008–11011. <https://doi.org/10.1021/jacs.7b05788>.
- (34) Moreira, L.; Calbo, J.; Calderon, R. M. K.; Santos, J.; Illescas, B. M.; Aragón, J.; Nierengarten, J.-F.; Guldi, D. M.; Ortí, E.; Martín, N. Unveiling the Nature of Supramolecular Crown Ether–C₆₀ Interactions. *Chem. Sci.* **2015**, *6* (8), 4426–4432. <https://doi.org/10.1039/C5SC00850F>.
- (35) Fuertes-Espinosa, C.; García-Simón, C.; Castro, E.; Costas, M.; Echegoyen, L.; Ribas, X. A Copper-Based Supramolecular Nanocapsule That Enables Straightforward Purification of Sc₃N-Based Endohedral Metallofullerene Soots. *Chem. – Eur. J.* **2017**, *23* (15), 3553–3557. <https://doi.org/10.1002/chem.201700046>.
- (36) Ke, X.-S.; Kim, T.; Lynch, V. M.; Kim, D.; Sessler, J. L. Flattened Calixarene-like Cyclic BODIPY Array: A New Photosynthetic Antenna Model. *J. Am. Chem. Soc.* **2017**, *139* (39), 13950–13956. <https://doi.org/10.1021/jacs.7b08611>.
- (37) Mahata, K.; Frischmann, P. D.; Würthner, F. Giant Electroactive M₄L₆ Tetrahedral Host Self-Assembled with Fe(II) Vertices and Perylene Bisimide Dye Edges. *J. Am. Chem. Soc.* **2013**, *135* (41), 15656–15661. <https://doi.org/10.1021/ja4083039>.
- (38) Shi, Y.; Cai, K.; Xiao, H.; Liu, Z.; Zhou, J.; Shen, D.; Qiu, Y.; Guo, Q.-H.; Stern, C.; Wasielewski, M. R.; et al. Selective Extraction of C₇₀ by a Tetragonal Prismatic Porphyrin Cage. *J. Am. Chem. Soc.* **2018**, *140* (42), 13835–13842. <https://doi.org/10.1021/jacs.8b08555>.
- (39) Iwamoto, T.; Watanabe, Y.; Sadahiro, T.; Haino, T.; Yamago, S. Size-Selective Encapsulation of C₆₀ by [10]Cycloparaphenylene: Formation of the Shortest Fullerene-Peapod. *Angew. Chem. Int. Ed.* **2011**, *50* (36), 8342–8344. <https://doi.org/10.1002/anie.201102302>.
- (40) Lhoták, P.; Kunderát, O. Fullerene Receptors Based on Calixarene Derivatives. In *Artificial Receptors for Chemical Sensors*; Wiley-Blackwell, **2010**; pp 249–272. <https://doi.org/10.1002/9783527632480.ch8>.
- (41) Pérez, E. M.; Martín, N. Curves Ahead: Molecular Receptors for Fullerenes Based on Concave–Convex Complementarity. *Chem. Soc. Rev.* **2008**, *37* (8), 1512–1519. <https://doi.org/10.1039/B802589B>.
- (42) Kishi, N.; Akita, M.; Yoshizawa, M. Selective Host–Guest Interactions of a Transformable Coordination Capsule/Tube with Fullerenes. *Angew. Chem. Int. Ed.* **2014**, *53* (14), 3604–3607. <https://doi.org/10.1002/anie.201311251>.
- (43) Nakamura, T.; Ube, H.; Miyake, R.; Shionoya, M. A C₆₀-Templated Tetrameric Porphyrin Barrel Complex via Zinc-Mediated Self-Assembly Utilizing Labile Capping Ligands. *J. Am. Chem. Soc.* **2013**, *135* (50), 18790–18793. <https://doi.org/10.1021/ja4110446>.
- (44) Tashiro, K.; Aida, T. Metalloporphyrin Hosts for Supramolecular Chemistry of Fullerenes. *Chem. Soc. Rev.* **2007**, *36* (2), 189–197. <https://doi.org/10.1039/B614883M>.
- (45) Stefankiewicz, A. R.; Tamanini, E.; Pantos, G. D.; Sanders, J. K. M. Proton-Driven Switching Between Receptors for C₆₀ and C₇₀. *Angew. Chem. Int. Ed.* **2011**, *50* (25), 5725–5728. <https://doi.org/10.1002/anie.201100806>.

- (46) Gil-Ramírez, G.; Karlen, S. D.; Shundo, A.; Porfyrakis, K.; Ito, Y.; Briggs, G. A. D.; Morton, J. J. L.; Anderson, H. L. A Cyclic Porphyrin Trimer as a Receptor for Fullerenes. *Org. Lett.* **2010**, *12* (15), 3544–3547. <https://doi.org/10.1021/ol101393h>.
- (47) Moreira, L.; Calbo, J.; Illescas, B. M.; Aragó, J.; Nierengarten, I.; Delavaux-Nicot, B.; Ortí, E.; Martín, N.; Nierengarten, J.-F. Metal-Atom Impact on the Self-Assembly of Cup-and-Ball Metalloporphyrin–Fullerene Conjugates. *Angew. Chem. Int. Ed.* **2015**, *54* (4), 1255–1260. <https://doi.org/10.1002/anie.201409487>.
- (48) Ogoshi, T.; Ueshima, N.; Sakakibara, F.; Yamagishi, T.; Haino, T. Conversion from Pillar[5]Arene to Pillar[6–15]Arenes by Ring Expansion and Encapsulation of C₆₀ by Pillar[n]Arenes with Nanosize Cavities. *Org. Lett.* **2014**, *16* (11), 2896–2899. <https://doi.org/10.1021/ol501039u>.
- (49) Yokoi, H.; Hiraoka, Y.; Hiroto, S.; Sakamaki, D.; Seki, S.; Shinokubo, H. Nitrogen-Embedded Buckybowl and Its Assembly with C₆₀. *Nat. Commun.* **2015**, *6*, 8215. <https://doi.org/10.1038/ncomms9215>.
- (50) Sun, W.; Wang, Y.; Ma, L.; Zheng, L.; Fang, W.; Chen, X.; Jiang, H. Self-Assembled Carcerand-like Cage with a Thermoregulated Selective Binding Preference for Purification of High-Purity C₆₀ and C₇₀. *J. Org. Chem.* **2018**, *83* (23), 14667–14675. <https://doi.org/10.1021/acs.joc.8b02674>.
- (51) Sun, Z.; Mio, T.; Okada, T.; Matsuno, T.; Sato, S.; Kono, H.; Isobe, H. Unbiased Rotational Motions of an Ellipsoidal Guest in a Tight Yet Pliable Host. *Angew. Chem. Int. Ed.* **2019**, *58* (7), 2040–2044. <https://doi.org/10.1002/anie.201812771>.
- (52) Selmani, S.; Schipper, D. J. π -Concave Hosts for Curved Carbon Nanomaterials. *Chem. – Eur. J.* **2019**, *25* (27), 6673–6692. <https://doi.org/10.1002/chem.201806134>.
- (53) Toyota, S.; Tsurumaki, E. Exploration of Nano-Saturns: A Spectacular Sphere–Ring Supramolecular System. *Chem. – Eur. J.* **2019**, *25* (28), 6878–6890. <https://doi.org/10.1002/chem.201900039>.
- (54) Canevet, D.; Pérez, E. M.; Martín, N. Wraparound Hosts for Fullerenes: Tailored Macrocycles and Cages. *Angew. Chem. Int. Ed.* **2011**, *50* (40), 9248–9259. <https://doi.org/10.1002/anie.201101297>.
- (55) García-Simón, C.; Costas, M.; Ribas, X. Metallosupramolecular Receptors for Fullerene Binding and Release. *Chem. Soc. Rev.* **2015**, *45* (1), 40–62. <https://doi.org/10.1039/C5CS00315F>.
- (56) Yokoi, H.; Hiroto, S.; Sakamaki, D.; Seki, S.; Shinokubo, H. Supramolecular Assemblies of a Nitrogen-Embedded Buckybowl Dimer with C₆₀. *Chem. Sci.* **2018**, *9* (4), 819–824. <https://doi.org/10.1039/C7SC04453D>.
- (57) Rosokha, S. V.; Kochi, J. K. Continuum of Outer- and Inner-Sphere Mechanisms for Organic Electron Transfer. Steric Modulation of the Precursor Complex in Paramagnetic (Ion-Radical) Self-Exchanges. *J. Am. Chem. Soc.* **2007**, *129* (12), 3683–3697. <https://doi.org/10.1021/ja069149m>.
- (58) Rosokha, S. V.; Kochi, J. K. Fresh Look at Electron-Transfer Mechanisms via the Donor/Acceptor Bindings in the Critical Encounter Complex. *Acc. Chem. Res.* **2008**, *41* (5), 641–653. <https://doi.org/10.1021/ar700256a>.
- (59) Guha, S.; Goodson, F. S.; Corson, L. J.; Saha, S. Boundaries of Anion/Naphthalenediimide Interactions: From Anion– π Interactions to Anion-Induced Charge-Transfer and Electron-Transfer Phenomena. *J. Am. Chem. Soc.* **2012**, *134* (33), 13679–13691. <https://doi.org/10.1021/ja303173n>.
- (60) Würthner, F.; Saha-Möller, C. R.; Fimmel, B.; Ogi, S.; Leowanawat, P.; Schmidt, D. Perylene Bisimide Dye Assemblies as Archetype Functional Supramolecular Materials. *Chem. Rev.* **2016**, *116* (3), 962–1052. <https://doi.org/10.1021/acs.chemrev.5b00188>.
- (61) Würthner, F. Perylene Bisimide Dyes as Versatile Building Blocks for Functional Supramolecular Architectures. *Chem. Commun.* **2004**, No. 14, 1564–1579. <https://doi.org/10.1039/B401630K>.
- (62) Spenst, P.; Würthner, F. Photo- and Redoxfunctional Cyclophanes, Macrocycles, and Catenanes Based on Aromatic Bisimides. *J. Photochem. Photobiol. C Photochem. Rev.* **2017**, *31*, 114–138. <https://doi.org/10.1016/j.jphotochemrev.2017.03.002>.
- (63) Barendt, T. A.; Ferreira, L.; Marques, I.; Félix, V.; Beer, P. D. Anion- and Solvent-Induced Rotary Dynamics and Sensing in a Perylene Diimide [3]Catenane. *J. Am. Chem. Soc.* **2017**, *139* (26), 9026–9037. <https://doi.org/10.1021/jacs.7b04295>.
- (64) Huang, C.; Barlow, S.; Marder, S. R. Perylene-3,4,9,10-Tetracarboxylic Acid Diimides: Synthesis, Physical Properties, and Use in Organic Electronics. *J. Org. Chem.* **2011**, *76* (8), 2386–2407. <https://doi.org/10.1021/jo2001963>.
- (65) Schwartz, P.-O.; Biniek, L.; Zaborova, E.; Heinrich, B.; Brinkmann, M.; Leclerc, N.; Méry, S. Perylenediimide-Based Donor–Acceptor Dyads and Triads: Impact of Molecular Architecture on Self-Assembling Properties. *J. Am. Chem. Soc.* **2014**, *136* (16), 5981–5992. <https://doi.org/10.1021/ja4129108>.
- (66) Dössel, L. F.; Kamm, V.; Howard, I. A.; Laquai, F.; Pisula, W.; Feng, X.; Li, C.; Takase, M.; Kudernac, T.; De Feyter, S.; et al. Synthesis and Controlled Self-Assembly of Covalently Linked Hexa-Peri-Hexabenzocoronene/Perylene Diimide Dyads as Models To Study Fundamental Energy and Electron Transfer Processes. *J. Am. Chem. Soc.* **2012**, *134* (13), 5876–5886. <https://doi.org/10.1021/ja211504a>.
- (67) Lee, K. J.; Woo, J. H.; Kim, E.; Xiao, Y.; Su, X.; Mazur, L. M.; Attias, A.-J.; Fages, F.; Cregut, O.; Barsella, A.; et al. Electronic Energy and Electron Transfer Processes in Photoexcited Donor–Acceptor Dyad and Triad Molecular Systems Based on Triphenylene and Perylene Diimide Units. *Phys. Chem. Chem. Phys.* **2016**, *18* (11), 7875–7887. <https://doi.org/10.1039/C5CP06279A>.

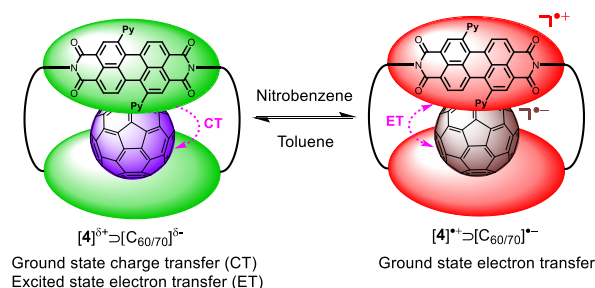
- (68) Wolf, M.; Ogawa, A.; Bechtold, M.; Vonesch, M.; Wytko, J. A.; Oohora, K.; Campidelli, S.; Hayashi, T.; Guldi, D. M.; Weiss, J. Light Triggers Molecular Shuttling in Rotaxanes: Control over Proximity and Charge Recombination. *Chem. Sci.* **2019**, *10* (13), 3846–3853. <https://doi.org/10.1039/C8SC05328F>.
- (69) Chamberlain, T. W.; Davies, E. S.; Khlobystov, A. N.; Champness, N. R. Multi-Electron-Acceptor Dyad and Triad Systems Based on Perylene Bisimides and Fullerenes. *Chem. – Eur. J.* **2011**, *17* (13), 3759–3767. <https://doi.org/10.1002/chem.201003092>.
- (70) Baffreau, J.; Leroy-Lhez, S.; Văn Anh, N.; Williams, R. M.; Hudhomme, P. Fullerene C60–Perylene-3,4:9,10-Bis(Dicarboximide) Light-Harvesting Dyads: Spacer-Length and Bay-Substituent Effects on Intramolecular Singlet and Triplet Energy Transfer. *Chem. – Eur. J.* **2008**, *14* (16), 4974–4992. <https://doi.org/10.1002/chem.200800156>.
- (71) Gómez, R.; Segura, J. L.; Martín, N. Highly Efficient Light-Harvesting Organofullerenes. *Org. Lett.* **2005**, *7* (4), 717–720. <https://doi.org/10.1021/ol047451z>.
- (72) Hua, J.; Meng, F.; Ding, F.; Li, F.; Tian, H. Novel Soluble and Thermally-Stable Fullerene Dyad Containing Perylene. *J. Mater. Chem.* **2004**, *14* (12), 1849–1853. <https://doi.org/10.1039/B316996K>.
- (73) Xiao, S.; Li, Y.; Li, Y.; Zhuang, J.; Wang, N.; Liu, H.; Ning, B.; Liu, Y.; Lu, F.; Fan, L.; et al. [60]Fullerene-Based Molecular Triads with Expanded Absorptions in the Visible Region: Synthesis and Photovoltaic Properties. *J. Phys. Chem. B* **2004**, *108* (43), 16677–16685. <https://doi.org/10.1021/jp0478413>.
- (74) Wang, N.; Li, Y.; He, X.; Gan, H.; Li, Y.; Huang, C.; Xu, X.; Xiao, J.; Wang, S.; Liu, H.; et al. Synthesis and Characterization of a Novel Electrical and Optical-Active Triads Containing Fullerene and Perylenebisimide Units. *Tetrahedron* **2006**, *62* (6), 1216–1222. <https://doi.org/10.1016/j.tet.2005.10.061>.
- (75) Baffreau, J.; Perrin, L.; Leroy-Lhez, S.; Hudhomme, P. Perylene-3,4:9,10-Bis(Dicarboximide) Linked to [60]Fullerene as a Light-Harvesting Antenna. *Tetrahedron Lett.* **2005**, *46* (27), 4599–4603. <https://doi.org/10.1016/j.tetlet.2005.04.132>.
- (76) Hua, J.; Meng, F.; Ding, F.; Tian, H. Novel Soluble and Thermally Stable Perylene Dye with Two [60] Fullerene Units. *Chem. Lett.* **2004**, *33* (4), 432–433. <https://doi.org/10.1246/cl.2004.432>.
- (77) Liu, Y.; Wang, N.; Li, Y.; Liu, H.; Li, Y.; Xiao, J.; Xu, X.; Huang, C.; Cui, S.; Zhu, D. A New Class of Conjugated Polyacetylenes Having Perylene Bisimide Units and Pendant Fullerene or Porphyrin Groups. *Macromolecules* **2005**, *38* (11), 4880–4887. <https://doi.org/10.1021/ma050434k>.
- (78) Li, Y.; Li, Y.; Liu, H.; Wang, S.; Wang, N.; Zhuang, J.; Li, X.; He, X.; Daoben Zhu. Self-Assembled Monolayers of Porphyrin–Perylenetetracarboxylic Diimide–[60] Fullerene on Indium Tin Oxide Electrodes: Enhancement of Light Harvesting in the Visible Light Region. *Nanotechnology* **2005**, *16* (9), 1899. <https://doi.org/10.1088/0957-4484/16/9/080>.
- (79) Feng, L.; Rudolf, M.; Wolfrum, S.; Troeger, A.; Slanina, Z.; Akasaka, T.; Nagase, S.; Martín, N.; Ameri, T.; Brabec, C. J.; et al. A Paradigmatic Change: Linking Fullerenes to Electron Acceptors. *J. Am. Chem. Soc.* **2012**, *134* (29), 12190–12197. <https://doi.org/10.1021/ja3039695>.
- (80) Shibano, Y.; Umeyama, T.; Matano, Y.; Tkachenko, N. V.; Lemmetyinen, H.; Imahori, H. Synthesis and Photophysical Properties of Electron-Rich Perylenediimide–Fullerene Dyad. *Org. Lett.* **2006**, *8* (20), 4425–4428. <https://doi.org/10.1021/ol061506a>.
- (81) Martín-Gomis, L.; Rotas, G.; Ohkubo, K.; Fernández-Lázaro, F.; Fukuzumi, S.; Tagmatarchis, N.; Sastre-Santos, Á. Does a Nitrogen Matter? Synthesis and Photoinduced Electron Transfer of Perylenediimide Donors Covalently Linked to C59N and C60 Acceptors. *Nanoscale* **2015**, *7* (16), 7437–7444. <https://doi.org/10.1039/C5NR00308C>.
- (82) Pla, S.; Niemi, M.; Martín-Gomis, L.; Fernández-Lázaro, F.; Lemmetyinen, H.; Tkachenko, N. V.; Sastre-Santos, Á. Charge Separation and Charge Recombination Photophysical Studies in a Series of Perylene–C60 Linear and Cyclic Dyads. *Phys. Chem. Chem. Phys.* **2016**, *18* (5), 3598–3605. <https://doi.org/10.1039/C5CP06340J>.
- (83) Baffreau, J.; Leroy-Lhez, S.; Hudhomme, P.; Groeneveld, M. M.; van Stokkum, I. H. M.; Williams, R. M. Superabsorbing Fullerenes: Spectral and Kinetic Characterization of Photoinduced Interactions in Perylenediimide–Fullerene–C60 Dyads. *J. Phys. Chem. A* **2006**, *110* (49), 13123–13125. <https://doi.org/10.1021/jp066415+>.
- (84) Pla, S.; Martín-Gomis, L.; Ohkubo, K.; Fukuzumi, S.; Fernández-Lázaro, F.; Sastre-Santos, Á. Macrocyclic Dyads Based on C60 and Perylenediimides Connected by Click Chemistry. *Asian J. Org. Chem.* **2014**, *3* (2), 185–197. <https://doi.org/10.1002/ajoc.201300235>.
- (85) Izquierdo, M.; Platzer, B.; Stasyuk, A. J.; Stasyuk, O. A.; Voityuk, A. A.; Cuesta, S.; Solà, M.; Guldi, D. M.; Martín, N. All-Fullerene Electron Donor–Acceptor Conjugates. *Angew. Chem. Int. Ed.* **2019**, *58* (21), 6932–6937. <https://doi.org/10.1002/anie.201901863>.
- (86) Liu, Y.; Xiao, S.; Li, H.; Li, Y.; Liu, H.; Lu, F.; Zhuang, J.; Zhu, D. Self-Assembly and Characterization of A Novel Hydrogen-Bonded Nanostructure. *J. Phys. Chem. B* **2004**, *108* (20), 6256–6260. <https://doi.org/10.1021/jp0373853>.
- (87) Hofmann, C. C.; Lindner, S. M.; Ruppert, M.; Hirsch, A.; Haque, S. A.; Thelakkat, M.; Köhler, J. Mutual Interplay of Light Harvesting and Triplet Sensitizing in a Perylene Bisimide Antenna–Fullerene Dyad. *J. Phys. Chem. B* **2010**, *114* (28), 9148–9156. <https://doi.org/10.1021/jp1035585>.

- (88) Shibano, Y.; Umeyama, T.; Matano, Y.; Tkachenko, N. V.; Lemmetyinen, H.; Araki, Y.; Ito, O.; Imahori, H. Large Reorganization Energy of Pyrrolidine-Substituted Perylenediimide in Electron Transfer. *J. Phys. Chem. C* **2007**, *111* (16), 6133–6142. <https://doi.org/10.1021/jp068893q>.
- (89) Zhao, Y.; Wasielewski, M. R. 3,4:9,10-Perylenebis(Dicarboximide) Chromophores That Function as Both Electron Donors and Acceptors. *Tetrahedron Lett.* **1999**, *40* (39), 7047–7050. [https://doi.org/10.1016/S0040-4039\(99\)01468-9](https://doi.org/10.1016/S0040-4039(99)01468-9).
- (90) Lukas, A. S.; Zhao, Y.; Miller, S. E.; Wasielewski, M. R. Biomimetic Electron Transfer Using Low Energy Excited States: A Green Perylene-Based Analogue of Chlorophyll a. *J. Phys. Chem. B* **2002**, *106* (6), 1299–1306. <https://doi.org/10.1021/jp014073w>.
- (91) Münich, P. W.; Schierl, C.; Dirian, K.; Volland, M.; Bauroth, S.; Wibmer, L.; Syrgiannis, Z.; Clark, T.; Prato, M.; Guldi, D. M. Tuning the Carbon Nanotube Selectivity: Optimizing Reduction Potentials and Distortion Angles in Perylenediimides. *J. Am. Chem. Soc.* **2018**, *140* (16), 5427–5433. <https://doi.org/10.1021/jacs.8b00452>.
- (92) Beauvilliers, E. E.; Topka, M. R.; Dinolfo, P. H. Synthesis and Characterization of Perylene Diimide Based Molecular Multilayers Using CuAAC: Towards Panchromatic Assemblies. *RSC Adv.* **2014**, *4* (62), 32866–32875. <https://doi.org/10.1039/C4RA04512B>.
- (93) Hancock, L. M.; Beer, P. D. Sodium and Barium Cation-Templated Synthesis and Cation-Induced Molecular Pirouetting of a Pyridine N-Oxide Containing [2]Rotaxane. *Chem. Commun.* **2011**, *47* (21), 6012–6014. <https://doi.org/10.1039/C1CC11224D>.
- (94) Saito, Y.; Matsumoto, K.; Bag, S. S.; Ogasawara, S.; Fujimoto, K.; Hanawa, K.; Saito, I. C8-Alkynyl- and Alkylamino Substituted 2'-Deoxyguanosines: A Universal Linker for Nucleic Acids Modification. *Tetrahedron* **2008**, *64* (16), 3578–3588. <https://doi.org/10.1016/j.tet.2008.01.091>.
- (95) Shibano, Y.; Umeyama, T.; Matano, Y.; Imahori, H. Electron-Donating Perylene Tetracarboxylic Acids for Dye-Sensitized Solar Cells. *Org. Lett.* **2007**, *9* (10), 1971–1974. <https://doi.org/10.1021/ol070556s>.
- (96) Seibt, J.; Marquetand, P.; Engel, V.; Chen, Z.; Dehm, V.; Würthner, F. On the Geometry Dependence of Molecular Dimer Spectra with an Application to Aggregates of Perylene Bisimide. *Chem. Phys.* **2006**, *328* (1), 354–362. <https://doi.org/10.1016/j.chemphys.2006.07.023>.
- (97) For $\lambda_{\text{abs,max}} A_{0-0}/A_{0-1} = 2$ indicating the absence of intermolecular or intramolecular aromatic stacking between PDIs in solution.⁹⁶
- (98) Ruoff, R. S.; Tse, D. S.; Malhotra, R.; Lorents, D. C. Solubility of Fullerene (C60) in a Variety of Solvents. *J. Phys. Chem.* **1993**, *97* (13), 3379–3383. <https://doi.org/10.1021/j100115a049>.
- (99) So that changes could be observed throughout the spectral window, the electronic spectra were corrected for absorbances from fullerenes at $\lambda < 600$ nm.
- (100) Calculated by integration of peak intensities from $\lambda_{\text{em}} = 700 - 850$ nm.
- (101) Iwamoto, T.; Slanina, Z.; Mizorogi, N.; Guo, J.; Akasaka, T.; Nagase, S.; Takaya, H.; Yasuda, N.; Kato, T.; Yamago, S. Partial Charge Transfer in the Shortest Possible Metallofullerene Peapod, La@C82@[11]Cycloparaphenylene. *Chem. – Eur. J.* **2014**, *20* (44), 14403–14409. <https://doi.org/10.1002/chem.201403879>.
- (102) <http://Supramolecular.org>.
- (103) Thordarson, P. Determining Association Constants from Titration Experiments in Supramolecular Chemistry. *Chem. Soc. Rev.* **2011**, *40* (3), 1305–1323. <https://doi.org/10.1039/C0CS00062K>.
- (104) Hibbert, D. B.; Thordarson, P. The Death of the Job Plot, Transparency, Open Science and Online Tools, Uncertainty Estimation Methods and Other Developments in Supramolecular Chemistry Data Analysis. *Chem. Commun.* **2016**, *52* (87), 12792–12805. <https://doi.org/10.1039/C6CC03888C>.
- (105) This region was also chosen because the absence of spectral overlap with fullerene bands permitted the use of non-corrected absorption spectra thus minimizing error. Non-sigmoidal residues and low fitting covariances indicate an appropriate binding model.^{103,104}
- (106) Tashiro, K.; Aida, T.; Zheng, J.-Y.; Kinbara, K.; Saigo, K.; Sakamoto, S.; Yamaguchi, K. A Cyclic Dimer of Metalloporphyrin Forms a Highly Stable Inclusion Complex with C60. *J. Am. Chem. Soc.* **1999**, *121* (40), 9477–9478. <https://doi.org/10.1021/ja992416m>.
- (107) Isla, H.; Gallego, M.; Pérez, E. M.; Viruela, R.; Ortí, E.; Martín, N. A Bis-ExTTF Macrocyclic Receptor That Associates C60 with Micromolar Affinity. *J. Am. Chem. Soc.* **2010**, *132* (6), 1772–1773. <https://doi.org/10.1021/ja910107m>.
- (108) Perturbations were too small to be accurately fitted.
- (109) Diao, G.; Li, L.; Zhang, Z. The Electrochemical Reduction of Fullerenes, C60 and C70. *Talanta* **1996**, *43* (10), 1633–1637. [https://doi.org/10.1016/0039-9140\(96\)01879-6](https://doi.org/10.1016/0039-9140(96)01879-6).
- (110) Nakamura, T.; Tsukuda, S.; Nabeshima, T. Double-Circularly Connected Saloph-Belt Macrocycles Generated from a Bis-Armed Bifunctional Monomer. *J. Am. Chem. Soc.* **2019**, *141* (16), 6462–6467. <https://doi.org/10.1021/jacs.9b00171>.
- (111) C₆₀ is nearly ten times more soluble in o-DCB than toluene.⁹⁸

- (112) Tsuchiya, T.; Wielopolski, M.; Sakuma, N.; Mizorogi, N.; Akasaka, T.; Kato, T.; Guldi, D. M.; Nagase, S. Stable Radical Anions Inside Fullerene Cages: Formation of Reversible Electron Transfer Systems. *J. Am. Chem. Soc.* **2011**, *133* (34), 13280–13283. <https://doi.org/10.1021/ja205391v>.
- (113) Indicative of a strong electronic component to the host–guest interaction with C₇₀.¹⁰¹
- (114) A higher concentration of C₆₀ guest was required to achieve similar $\Delta\delta$ in this more competitive solvent.
- (115) Saegusa, Y.; Ishizuka, T.; Kojima, T.; Mori, S.; Kawano, M.; Kojima, T. Supramolecular Interaction of Fullerenes with a Curved π -Surface of a Monomeric Quadruply Ring-Fused Porphyrin. *Chem. – Eur. J.* **2015**, *21* (14), 5302–5306. <https://doi.org/10.1002/chem.201500389>.
- (116) Gallego, M.; Calbo, J.; Krick Calderon, R. M.; Pla, P.; Hsieh, Y.-C.; Pérez, E. M.; Wu, Y.-T.; Ortí, E.; Guldi, D. M.; Martín, N. Complexation and Electronic Communication between Corannulene-Based Buckybowls and a Curved Truxene-TTF Donor. *Chem. – Eur. J.* **2017**, *23* (15), 3666–3673. <https://doi.org/10.1002/chem.201604921>.
- (117) The twisted PDI framework appears to allow some of the protons to be directed towards the fullerene cage.
- (118) Hung, R. R.; Grabowski, J. J. A Precise Determination of the Triplet Energy of Carbon (C₆₀) by Photoacoustic Calorimetry. *J. Phys. Chem.* **1991**, *95* (16), 6073–6075. <https://doi.org/10.1021/j100169a007>.
- (119) Kandrashkin, Y. E.; van der Est, A. Time-Resolved EPR Spectroscopy of Photosynthetic Reaction Centers: From Theory to Experiment. *Appl. Magn. Reson.* **2007**, *31* (1), 105–122. <https://doi.org/10.1007/BF03166250>.
- (120) Maeda, K.; Storey, J. G.; Liddell, P. A.; Gust, D.; Hore, P. J.; Wedge, C. J.; Timmel, C. R. Probing a Chemical Compass: Novel Variants of Low-Frequency Reaction Yield Detected Magnetic Resonance. *Phys. Chem. Chem. Phys.* **2015**, *17* (5), 3550–3559. <https://doi.org/10.1039/C4CP04095C>.
- (121) Stronger binding in nitrobenzene made a 1:1 host–guest stoichiometric model a superior fit than a 1:2 model. This was confirmed by Job Plot analysis (Figure S8.1).
- (122) By comparison to the electronic absorption spectrum of an electrochemically⁹⁰ and photochemically⁸⁰ generated [PDI]⁺.
- (123) Giaimo, J. M.; Gusev, A. V.; Wasielewski, M. R. Excited-State Symmetry Breaking in Cofacial and Linear Dimers of a Green Perylenediimide Chlorophyll Analogue Leading to Ultrafast Charge Separation. *J. Am. Chem. Soc.* **2002**, *124* (29), 8530–8531. <https://doi.org/10.1021/ja026422l>.
- (124) van der Boom, T.; Hayes, R. T.; Zhao, Y.; Bushard, P. J.; Weiss, E. A.; Wasielewski, M. R. Charge Transport in Photofunctional Nanoparticles Self-Assembled from Zinc 5,10,15,20-Tetrakis(Perylenediimide)Porphyrin Building Blocks. *J. Am. Chem. Soc.* **2002**, *124* (32), 9582–9590. <https://doi.org/10.1021/ja026286k>.
- (125) Connelly, N. G.; Geiger, W. E. Chemical Redox Agents for Organometallic Chemistry. *Chem. Rev.* **1996**, *96* (2), 877–910. <https://doi.org/10.1021/cr940053x>.
- (126) Ito, O. Photoinduced Electron Transfer of Fullerenes (C₆₀ and C₇₀) Studied by Transient Absorption Measurements in near-IR Region. *Res. Chem. Intermed.* **1997**, *23* (5), 389–402. <https://doi.org/10.1163/156856797X00141>.
- (127) Cataldo, F.; Iglesias-Groth, S.; Manchado, A. On the Radical Anion Spectra of Fullerenes C₆₀ and C₇₀. *Fuller. Nanotub. Carbon Nanostructures* **2013**, *21* (6), 537–548. <https://doi.org/10.1080/1536383X.2011.643422>.
- (128) Isobe, H.; Tanaka, T.; Nakanishi, W.; Lemiègre, L.; Nakamura, E. Regioselective Oxygenative Tetraamination of [60]Fullerene. Fullerene-Mediated Reduction of Molecular Oxygen by Amine via Ground State Single Electron Transfer in Dimethyl Sulfoxide. *J. Org. Chem.* **2005**, *70* (12), 4826–4832. <https://doi.org/10.1021/jo050432y>.
- (129) Stinchcombe, J.; Penicaud, A.; Bhyrappa, P.; Boyd, P. D. W.; Reed, C. A. Buckminsterfulleride(1-) Salts: Synthesis, EPR, and the Jahn-Teller Distortion of C₆₀-. *J. Am. Chem. Soc.* **1993**, *115* (12), 5212–5217. <https://doi.org/10.1021/ja00065a037>.
- (130) Whilst no evidence for doubly oxidized or reduced PDI/C₆₀ species was found in the 1:1 host–guest stoichiometric complex [4]⊃[C₆₀] (Figure S4.9), a comparison to the green box Vis–NIR spectrum generated with two equivalents of Cu(II) triflate, indicates partial oxidation of a second PDI panel of the Green Box can occur in the presence of a large excess of guest (60 equiv., Figure S4.10). However, as before, there is only weak association with the second fullerene since titration data fitting to a 1:2 host–guest model reveals $K_{a2} \ll K_{a1}$.
- (131) Eaton, S. S.; Eaton, G. R. EPR Spectra of C₆₀ Anions. *Appl. Magn. Reson.* **1996**, *11* (2), 155–170. <https://doi.org/10.1007/BF03162051>.
- (132) Greaney, M. A.; Gorun, S. M. Production, Spectroscopy and Electronic Structure of Soluble Fullerene Ions. *J. Phys. Chem.* **1991**, *95* (19), 7142–7144. <https://doi.org/10.1021/j100172a012>.
- (133) Douthwaite, R. E.; Brough, A. R.; Green, M. L. H. Synthesis and Characterisation of NaC₆₀·5thf. *J. Chem. Soc. Chem. Commun.* **1994**, 0 (3), 267–268. <https://doi.org/10.1039/C39940000267>.
- (134) Krusic, P. J.; Wasserman, E.; Parkinson, B. A.; Malone, B.; Holler, E. R.; Keizer, P. N.; Morton, J. R.; Preston, K. F. Electron Spin Resonance Study of the Radical Reactivity of C₆₀. *J. Am. Chem. Soc.* **1991**, *113* (16), 6274–6275. <https://doi.org/10.1021/ja00016a056>.
- (135) Tsuchiya, T.; Sato, K.; Kurihara, H.; Wakahara, T.; Maeda, Y.; Akasaka, T.; Ohkubo, K.; Fukuzumi, S.; Kato, T.; Nagase, S. Spin-Site Exchange System Constructed from Endohedral Metallofullerenes and Organic Donors. *J. Am. Chem. Soc.* **2006**, *128* (45), 14418–14419. <https://doi.org/10.1021/ja062634x>.

- (136) Park, J. S.; Karnas, E.; Ohkubo, K.; Chen, P.; Kadish, K. M.; Fukuzumi, S.; Bielawski, C. W.; Hudnall, T. W.; Lynch, V. M.; Sessler, J. L. Ion-Mediated Electron Transfer in a Supramolecular Donor-Acceptor Ensemble. *Science* **2010**, 329 (5997), 1324–1327. <https://doi.org/10.1126/science.1192044>.
- (137) There is a documented affinity for EMFs with solvents such as pyridine and DMF due to an interaction with the basic N atom.
- (138) Tsuchiya, T.; Sato, K.; Kurihara, H.; Wakahara, T.; Nakahodo, T.; Maeda, Y.; Akasaka, T.; Ohkubo, K.; Fukuzumi, S.; Kato, T.; et al. Host–Guest Complexation of Endohedral Metallofullerene with Azacrown Ether and Its Application. *J. Am. Chem. Soc.* **2006**, 128 (20), 6699–6703. <https://doi.org/10.1021/ja0608390>.
- (139) Pérez, E. M.; Sánchez, L.; Fernández, G.; Martín, N. ExTTF as a Building Block for Fullerene Receptors. Unexpected Solvent-Dependent Positive Homotropic Cooperativity. *J. Am. Chem. Soc.* **2006**, 128 (22), 7172–7173. <https://doi.org/10.1021/ja0621389>.
- (140) Nielsen, K. A.; Cho, W.-S.; Sarova, G. H.; Petersen, B. M.; Bond, A. D.; Becher, J.; Jensen, F.; Guldi, D. M.; Sessler, J. L.; Jeppesen, J. O. Supramolecular Receptor Design: Anion-Triggered Binding of C₆₀. *Angew. Chem. Int. Ed.* **2006**, 45 (41), 6848–6853. <https://doi.org/10.1002/anie.200602724>.
- (141) Boyd, P. D. W.; Reed, C. A. Fullerene–Porphyrin Constructs. *Acc. Chem. Res.* **2005**, 38 (4), 235–242. <https://doi.org/10.1021/ar040168f>.
- (142) Electron transfer may also be assisted by the formation of fullerene aggregates in nitrobenzene (Figure S7.4), since this has been shown to lower their reduction potential.³³
- (143) Tsuchiya, T.; Kurihara, H.; Sato, K.; Wakahara, T.; Akasaka, T.; Shimizu, T.; Kamigata, N.; Mizorogi, N.; Nagase, S. Supramolecular Complexes of La@C₈₂ with Unsaturated Thiocrown Ethers. *Chem. Commun.* **2006**, 0 (34), 3585–3587. <https://doi.org/10.1039/B060183D>.
- (144) Schilder, A.; Gotschy, B.; Seidl, A.; Gompper, R. Preparation and Characterisation of the C₆₀ Charge Transfer Complex C₆₀–[1,1',3,3'-Tetramethyl-Δ^{2,2'}-Bi(Imidazolidine)]⁺. *Chem. Phys.* **1995**, 193 (3), 321–326. [https://doi.org/10.1016/0301-0104\(95\)00013-E](https://doi.org/10.1016/0301-0104(95)00013-E).
- (145) Klos, H.; Rystau, I.; Schütz, W.; Gotschy, B.; Skiebe, A.; Hirsch, A. Doping of C₆₀ with Tertiary Amines: TDAE, DBU, DBN. A Comparative Study. *Chem. Phys. Lett.* **1994**, 224 (3), 333–337. [https://doi.org/10.1016/0009-2614\(94\)00550-8](https://doi.org/10.1016/0009-2614(94)00550-8).
- (146) Therefore, our experimentation can be conducted over several hours without any significant effects from charge recombination. By contrast some of the longest reported lifetimes of photoinduced charge separated states in fullerene dyads are in the μs regime.
- (147) With a caveat that if the steric hindrance of the donor is too large it reduces the efficiency of SET to C₆₀,¹¹² meaning that Green Box appears to sit between these two extremes.
- (148) Konishi, T.; Ikeda, A.; Kishida, T.; Rasmussen, B. S.; Fujitsuka, M.; Ito, O.; Shinkai, S. Photoinduced Electron Transfer between C₆₀-Pendant Calixarene and Captured Electron Donor: Improvement of Electron-Transfer Efficiency by Applying Host–Guest Chemistry. *J. Phys. Chem. A* **2002**, 106 (43), 10254–10260. <https://doi.org/10.1021/jp021305y>.
- (149) Prylutskyy, Y. I.; Buchelnikov, A. S.; Voronin, D. P.; Kostjukov, V. V.; Ritter, U.; Parkinson, J. A.; Evstigneev, M. P. C₆₀ Fullerene Aggregation in Aqueous Solution. *Phys. Chem. Chem. Phys.* **2013**, 15 (23), 9351–9360. <https://doi.org/10.1039/C3CP50187F>.
- (150) Montero-Alejo, A. L.; Menéndez-Proupin, E.; Fuentes, M. E.; Delgado, A.; Montforts, F.-P.; Montero-Cabrera, L. A.; Vega, J. M. G. de la. Electronic Excitations of C₆₀ Aggregates. *Phys. Chem. Chem. Phys.* **2012**, 14 (37), 13058–13066. <https://doi.org/10.1039/C2CP41979C>.
- (151) Gaussian 09, M. J. Frisch, G. W. Trucks, H. B. Schlegel, G. E. Scuseria, M. A. Robb, J. R. Cheeseman, G. Scalmani, V. Barone, G. A. Petersson, H. Nakatsuji, X. Li, M. Caricato, A. Marenich, J. Bloino, B. G. Janesko, R. Gomperts, B. Mennucci, H. P. Hratchian, J. V. Ortiz, A. F. Izmaylov, J. L. Sonnenberg, D. Williams-Young, F. Ding, F. Lipparini, F. Egidi, J. Goings, B. Peng, A. Petrone, T. Henderson, D. Ranasinghe, V. G. Zakrzewski, J. Gao, N. Rega, G. Zheng, W. Liang, M. Hada, M. Ehara, K. Toyota, R. Fukuda, J. Hasegawa, M. Ishida, T. Nakajima, Y. Honda, O. Kitao, H. Nakai, T. Vreven, K. Throssell, J. A. Montgomery, Jr., J. E. Peralta, F. Ogliaro, M. Bearpark, J. J. Heyd, E. Brothers, K. N. Kudin, V. N. Staroverov, T. Keith, R. Kobayashi, J. Normand, K. Raghavachari, A. Rendell, J. C. Burant, S. S. Iyengar, J. Tomasi, M. Cossi, J. M. Millam, M. Klene, C. Adamo, R. Cammi, J. W. Ochterski, R. L. Martin, K. Morokuma, O. Farkas, J. B. Foresman, and D. J. Fox, Gaussian, Inc., Wallingford CT, 2009.
- (152) Marenich, A. V.; Cramer, C. J.; Truhlar, D. G. Universal Solvation Model Based on Solute Electron Density and on a Continuum Model of the Solvent Defined by the Bulk Dielectric Constant and Atomic Surface Tensions. *J. Phys. Chem. B* **2009**, 113 (18), 6378–6396. <https://doi.org/10.1021/jp810292n>.
- (153) Dawe, L. N.; AlHujran, T. A.; Tran, H.-A.; Mercer, J. I.; Jackson, E. A.; Scott, L. T.; Georgiou, P. E. Corannulene and Its Penta-Tert-Butyl Derivative Co-Crystallize 1 : 1 with Pristine C₆₀-Fullerene. *Chem. Commun.* **2012**, 48 (45), 5563–5565. <https://doi.org/10.1039/C2CC30652B>.
- (154) Yang, Y.; Cheng, K.; Lu, Y.; Ma, D.; Shi, D.; Sun, Y.; Yang, M.; Li, J.; Wei, J. A Polyaromatic Nano-Nest for Hosting Fullerenes C₆₀ and C₇₀. *Org. Lett.* **2018**, 20 (8), 2138–2142. <https://doi.org/10.1021/acs.orglett.8b00306>.

- (155) Xu, Y.-Y.; Tian, H.-R.; Li, S.-H.; Chen, Z.-C.; Yao, Y.-R.; Wang, S.-S.; Zhang, X.; Zhu, Z.-Z.; Deng, S.-L.; Zhang, Q.; et al. Flexible Decapyrrylcorannulene Hosts. *Nat. Commun.* **2019**, *10* (1), 1–9. <https://doi.org/10.1038/s41467-019-08343-6>.
- (156) Bhatta, R. S.; Iyer, P. P.; Dhinojwala, A.; Tsige, M. A Brief Review of Badger–Bauer Rule and Its Validation from a First-Principles Approach. *Mod. Phys. Lett. B* **2014**, *28* (29), 1430014. <https://doi.org/10.1142/S0217984914300142>.
- (157) Riley, K. E.; Merz, K. M. Insights into the Strength and Origin of Halogen Bonding: The Halobenzene–Formaldehyde Dimer. *J. Phys. Chem. A* **2007**, *111* (9), 1688–1694. <https://doi.org/10.1021/jp066745u>.
- (158) The energy difference between the two macrocyclic conformations ($\Delta E_{conf,4}$) is 15.1 (toluene) and 16.7 kcal mol⁻¹ (nitrobenzene). These energy differences should be carefully considered, since they do not include the Zero-Point Energy Correction (ZPVE). See Supporting Information section 10 for more details.
- (159) ZPVE or entropic effects were not considered in this energetic analysis.
- (160) Iwamoto, T.; Watanabe, Y.; Takaya, H.; Haino, T.; Yasuda, N.; Yamago, S. Size- and Orientation-Selective Encapsulation of C70 by Cycloparaphenylenes. *Chem. – Eur. J.* **2013**, *19* (42), 14061–14068. <https://doi.org/10.1002/chem.201302694>.
- (161) Pérez, E. M.; Martín, N. Molecular Tweezers for Fullerenes. *Pure Appl. Chem.* **2010**, *82* (3), 523–533. <https://doi.org/10.1351/PAC-CON-09-09-27>.
- (162) Utschig, L. M.; Thurnauer, M. C. Metal Ion Modulated Electron Transfer in Photosynthetic Proteins. *Acc. Chem. Res.* **2004**, *37* (7), 439–447. <https://doi.org/10.1021/ar020197v>.
- (163) Fukuzumi, S. Roles of Metal Ions in Controlling Bioinspired Electron-Transfer Systems. Metal Ion-Coupled Electron Transfer. In *Progress in Inorganic Chemistry*; Wiley-Blackwell, **2009**; pp 49–154. <https://doi.org/10.1002/9780470440124.ch2>.
- (164) Ferreira, K. N.; Iverson, T. M.; Maghlaoui, K.; Barber, J.; Iwata, S. Architecture of the Photosynthetic Oxygen-Evolving Center. *Science* **2004**, *303* (5665), 1831–1838. <https://doi.org/10.1126/science.1093087>.



Authors are required to submit a graphic entry for the Table of Contents (TOC) that, in conjunction with the manuscript title, should give the reader a representative idea of one of the following: A key structure, reaction, equation, concept, or theorem, etc., that is discussed in the manuscript. Consult the journal's Instructions for Authors for TOC graphic specifications.

Insert Table of Contents artwork here